

UC Berkeley

UC Berkeley Electronic Theses and Dissertations

Title

Discovery and Investigation of Small Molecule Inhibitors of Sulfate Assimilation Pathway as Novel Anti-Latent Tuberculosis Therapy

Permalink

<https://escholarship.org/uc/item/5zf006zb>

Author

Hsieh, Andy

Publication Date

2012

Peer reviewed|Thesis/dissertation

Discovery and Investigation of Small Molecule Inhibitors of Sulfate Assimilation
Pathway as Novel Anti-Latent Tuberculosis Therapy

by

Andy Hsieh

A dissertation submitted in partial satisfaction of the

requirements for the degree of

Doctor of Philosophy

in

Chemistry

in the

Graduate Division

of the

University of California, Berkeley

Committee in charge:

Professor Carolyn R. Bertozzi, Chair

Professor Matthew B. Francis

Professor Gregory M. Barton

Spring 2012

Abstract

Discovery and Investigation of Small Molecule Inhibitors of Sulfate Assimilation Pathway as Novel Anti-Latent Tuberculosis Therapy

by

Andy Hsieh

Doctor of Philosophy in Chemistry

University of California, Berkeley

Professor Carolyn R. Bertozzi, Chair

Mycobacterium tuberculosis (*Mtb*), the causative agent of tuberculosis (TB), is the single most deadly pathogen. An estimated 2 billion people are currently infected and 2 million die each year as a result of the disease. However, only 10% of the cases are symptomatic. Majority of the infections are latent, which is characterized by non-replicative, slow metabolic, and dormant *Mtb* surrounded by a plethora of immune called the granuloma in the lungs.

The nonreplicating persistent state of infection poses a great challenge to the efforts to eradicate TB. The frontline drugs, which were discovered almost half a century ago, are primarily efficacious against actively dividing or metabolically active bacilli. To ensure the latent infection would not transition into active infection, in a process called reactivation, the drugs are to be administered up to 9 months. The long regimen leads to high non-compliance rates and directly fuels the appearance of multiple drug-resistant (MDR), extensively drug-resistant (XDR), and just recently, the discovery of totally drug-resistant (TDR) TB. To complicate matters, the co-infection with HIV promotes the progression to AIDS and animate dormancy to active infections. Unfortunately, due to the lack of financial incentive, TB research in pharmaceutical industry has largely been absent. The responsibility falls in the hands of academic labs to discover new drugs that can target *Mtb* in the latent phase to eliminate the episode of reactivation, shorten the regimen, and increase compliancy.

This thesis presents the utilization of high-throughput screening in an effort to identify small molecule inhibitors that target the sulfate assimilation pathway, which is believed to be critical during the latent phase of TB infection. Chapter 1 reviews the molecular pathways that govern the sulfate assimilation pathway. Chapter 2 discusses the efforts of devising an assay amenable to high throughput screening, target production, library selection, and quality control. Chapter 3 presents follow-up studies that

encompass the confirmation of hit compounds, the elimination of aggregate formers, and elucidation of the binding mechanism. In addition, structure activity relationship was investigated by testing compounds similar in structure to the most potent compounds. Finally, chapter 4 explores the *in vivo* activity of the lead compounds in growth inhibition of *Mycobacterium tuberculosis*, *Escherichia coli*, and *Bacillus subtilis*, as well as toxicity profile against mammalian cell line.

This dissertation is dedicated to my family and friends.

Discovery and Investigation of Small Molecule Inhibitors of Sulfate Assimilation
Pathway as Novel Anti-Latent Tuberculosis Therapy

Table of Contents

List of Figures	x
List of Tables	x
List of Schemes	x
Acknowledgements	x

Chapter 1. The role of sulfur metabolism in the pathogenesis of *Mycobacterium tuberculosis* and the potential for therapeutic avenues

Introduction	1
The role of sulfated metabolites in the pathogenesis of <i>Mtb</i>	2
The sulfate assimilation pathway in <i>Mtb</i>	3
Regulation of sulfur metabolism genes in facilitating bacteria adaptation	4
Small molecule inhibition of enzymes in the sulfate assimilation pathway	
Sulfation branch	5
Reductive branch	5
Summary	6
Thesis overview	6
References	6

Chapter 2. High throughput screening of small molecule inhibitors of *Mtb* ATP sulfurylase

Introduction	12
--------------	----

Heterologous expression of <i>Mtb</i> ATP sulfurylase	14
<i>Mtb</i> ATP sulfurylase forms complex oligomers	16
Luciferase-based assay is amenable to high throughput screening	17
Determining the linear range of ATP consumption activity of <i>Mtb</i> ATP sulfurylase	18
High throughput screening of small molecule inhibitors of the <i>Mtb</i> sulfation pathway	19
Conclusions	26
Materials and Methods	27
References	29

Chapter 3. Validation and characterization of hit compounds that inhibit *Mtb* ATP sulfurylase

Introduction	33
Identification of aggregate forming small molecules among the hit compounds	35
Lead compounds are discriminatory against eukaryotic ATP sulfurylase	43
Analyzing the structure activity relationship by probing derivatives of the lead compounds	
Structure activity relationship of compound 1	43
Structure activity relationship of compound 3	45
Materials and Methods	46
References	48

Chapter 4. Characterization of the lead compounds' *in vivo* activity and specificity against *Mtb* and other pathogenic bacteria

Introduction	50
Compounds 1 and 2 exhibit cytotoxicity in Vero cell line	50
Lead compounds do not inhibit growth of <i>Saccharomyces cerevisiae</i> below 2 mM	51
<i>In vivo</i> inhibitory activity against Gram negative pathogen <i>E. coli</i> and Gram positive pathogen <i>Bacillus subtilis</i>	52
<i>In vivo</i> inhibitory activity against <i>Mtb</i>	53
Conclusions	54
Materials and Methods	55
References	56

List of Figures

Figure 1-1	Sulfur-containing metabolites in <i>Mtb</i>	2
Figure 1-2	Sulfate assimilation pathway of <i>Mtb</i>	3
Figure 2-1	Sulfate assimilation pathway of <i>Mtb</i>	13
Figure 2-2	Western blot analysis detects the presence of two His ₆ -tagged proteins	14
Figure 2-3	Mass spectra confirm the identity of the CysNC and CysD subunits	15
Figure 2-4	Analytical centrifugation reveals <i>Mtb</i> ATP sulfurylase forms complex oligomers	16
Figure 2-5	Luciferase assay is used to assess <i>Mtb</i> ATP sulfurylase activity	18

Figure 2-6	Reaction progress curve for determining the linear range of <i>Mtb</i> ATP sulfurylase	19
Figure 3-1	Structures of the <i>mant</i> -nucleotide analogs	33
Figure 3-2	Compounds that show competitive inhibition against <i>Mtb</i> ATP sulfurylase	41
Figure 3-3	Competitive binding assay elucidates the binding sites of the 6 lead compounds	42
Figure 4-1	Cytotoxicity of the 6 lead compounds	51
Figure 4-2	Lead compounds do not inhibit growth of <i>Saccharomyces cerevisiae</i> culture less than 2 mM	51
Figure 4-3	The growth inhibitory activity of the lead compounds against <i>E. coli</i> is inconclusive.	52
Figure 4-4	The growth inhibitory activity of the lead compounds against <i>B. subtilis</i> is inconclusive.	53
Figure 4-5	Lead compounds 1 and 5 inhibit growth of <i>Mtb</i> cultures at 125 μ M and 500 μ M, respectively.	

List of Tables

Table 2-1	Parameters of the high throughput screening of <i>Mtb</i> ATP sulfurylase	20
Table 2-2	Structures, Lipinski parameters, and percent inhibition of the 45 hit compounds	21
Table 3-1	Determination of the aggregate forming propensities of the hit compounds by measuring IC ₅₀ values at different enzyme concentrations	35
Table 3-2	GTP antagonists exhibit selectivity for prokaryotic homologs ATP sulfurylase	43

List of Schemes

Scheme 1-1	Pathogenesis of tuberculosis	1
Scheme 2-1	Luciferase hydrolyzes ATP to produce luminescence	17
Scheme 3-1	Nucleotide pocket binding competition assay	34

Acknowledgements

I am truly grateful to everyone who has positively impacted my graduate education at UC Berkeley. First and foremost, I want to express my heartfelt gratitude to Professor Carolyn Bertozzi. Carolyn has been an inspirational advisor and outstanding teacher over the past six years. She has built a wonderful environment to conduct ground breaking research that challenges the *status quo*. I have the utmost respect for her insightful knowledge, creativity, and constructive advice as a researcher. She also puts in countless hours in the professional development of students (There are 8 students in our class, and that translates into 24 mock qualifier exam sessions). In short, she is the best graduate advisor that one could have wished for.

This dissertation is the culmination of several collaborations. I had the unique opportunity to work with the Protein Chemistry Group at Gilead Sciences. Visiting the research facility was an eye opening experience as a first year graduate student, but more importantly, I gained insight about how the biotech industry conducts research. One of the most intriguing results that came from this fruitful collaboration was the characterization and expression of *Mtb* ATP sulfurylase, and its formation of complex oligomers. Not only they saved approximately six to nine months (coincidentally, this is the length of drug-sensitive TB regimen) of my graduate career, it also opened new research avenues that we could pursue in the future.

More recently, I have been working closely with Dr. Kim Sogi (updated 5/1/2012) on the investigation of the lead compounds' *in vivo* potency. Without her expertise in microbiology, especially dealing with potentially hazardous pathogens in BSL3 facility, the data could not have been obtained. She also taught me the ins and outs of the art of sterile technique in the TC room. I am especially grateful for her exceptional organizational skills both during this collaboration and overseeing the completion of the 2010 "Chemical Mycobacteriology" grant proposal.

I also would like to thank people who have helped me to get started in this lab. Dr. Jason Rush, who has the famous "sexy ninja body", had always been a source of information and solution in enzymology and physical organic chemistry. I also want to thank Dr. Brian Carlson, who knew pretty much everything about biology, taught me protein expression and purification. I also learned a lot from and enjoyed being in the TB-subgroup. I would like to acknowledge Dr. Stavroula Hatzios, who is one of the most talented scientist that I had the pleasure to meet and interact.

I was fortunate enough to join the Bertozzi Lab with 7 other wonderful scientists. In the midst of taking classes, first year report, GRS, and the qualifier exam, it's always good to have people to can relate what I was going through. I want to thank Dr. Sonny Hsiao for being a great friend and collaborator. My graduate career would not have been the same without you.

The Bertozzi Lab is blessed with the super support staff: Karen Carkuff, Asia Avelino, Olga Martinez, Dr. Sia Kruschke, and Dr. Cheryl McVaugh. From ordering lab supplies, travel arrangements, or just chitchatting, they're instrumental for making sure the non-science part of the lab is functional.

Outside of lab, I have spent a lot of time with the Berkeley Association of Taiwanese Students (BATS) tennis team. I thank my best friend and teammate, Wei-

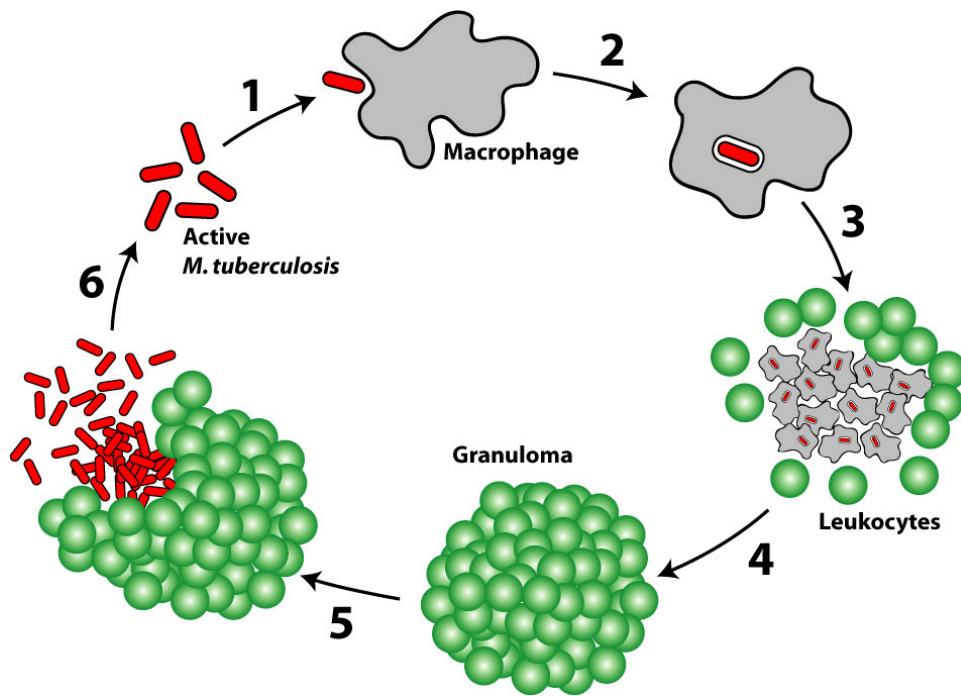
Chun Kao, for his friendship and support through thick and thin. I admire his strong will, determination, persistence, and “leave everything on the court” approach to life. He is the “older brother” that I never had.

Lastly, I want to close by thanking my family. I thank my Dad, who inspired me to pursue a career as a scientist; and my Mom, who instilled a bit of humor in me, which is much needed in the path of becoming a scientist. Most importantly, you taught me the meaning of unconditional love. You gave me support and encouragement when I needed the most. I can only wish that one day, I can repay everything you have given to me.

Chapter 1: The role of sulfur metabolism in the pathogenesis of *Mycobacterium tuberculosis* and the potential for therapeutic avenues

Introduction

Mycobacterium tuberculosis (*Mtb*), the causative agent of tuberculosis (TB) is the world's single most deadly human pathogen and poses a grave threat to global health. It is estimated that one-third of the world's population is infected with *Mtb* and 2 million die each year as a result of the disease [1]. The difficulties in treating infections are stemmed from the requirement of multiple drugs administered over 6 to 9 months [2], the emergence of multidrug-resistant strains [3], and unique feature of the disease progression within human hosts.



SCHEME 1-1. Pathogenesis of tuberculosis. 1) Active *Mtb* is inhaled and situated in the alveoli of the lungs. 2) A resident macrophage phagocytoses the *Mtb* bacterium upon detection. 3) *Mtb* has evolved an elaborate mechanism to arrest the maturation and acidification of the phagosomal compartment. The persistent stimuli from the infection encourage the recruitment of leukocytes to the site. 4) As the increasing number of leukocytes aggregate around infected macrophages, a structure called the granuloma is formed. The granuloma is a dynamic mass of immune cells that can maintain its integrity for years in the host. 5) In certain situations, such as coinfection with HIV, drug use, or aging, the equilibrium is compromised, causing reactivation of *Mtb*, and thereby initiating a new round of infection.

Infection begins with the entry of *Mtb* into the lungs (**Step 1, Scheme 1-1**) and phagocytosis by resident alveolar macrophages [4] (**Step 2**). Once therein, *Mtb* disrupts the normal maturation of phagosomes into phagolysosomes, inhibits the acidification and activation of lytic enzymes, and replicates within the altered phagosomal compartment [5] (**Step 3**). The host responds by recruitment of leukocytes that surround and seclude the infected macrophages in a structure called a granuloma [6] (**Step 4**). The confined microenvironment that is deprived of nutrients and oxygen induces *Mtb* to transition into a low-metabolic, non-replicating state, which can persist for years or decades [7] (**Step 5**). This stage is known as the latent phase of infection or latency. The breakdown of this metastable equilibrium of immune containment (*e.g.*, via reduced immune capacity associated with aging, HIV coinfection, and immunosuppressant treatment, *etc.*) causes the reactivation of *Mtb* replication and progression into active infection (**Step 6**). Given that the vast majority of infected individuals harbor latent *Mtb* – a state that is refractory to all known treatments – there is a considerable interest in understanding the molecular mechanisms underlying entry into, survival during, and exit from latency [5]. Enzymes and pathways that are critical for latency may serve as targets for anti-tuberculosis drugs that treat a major patient population whose needs are presently unmet.

The role of sulfated metabolites in the pathogenesis of *Mtb*

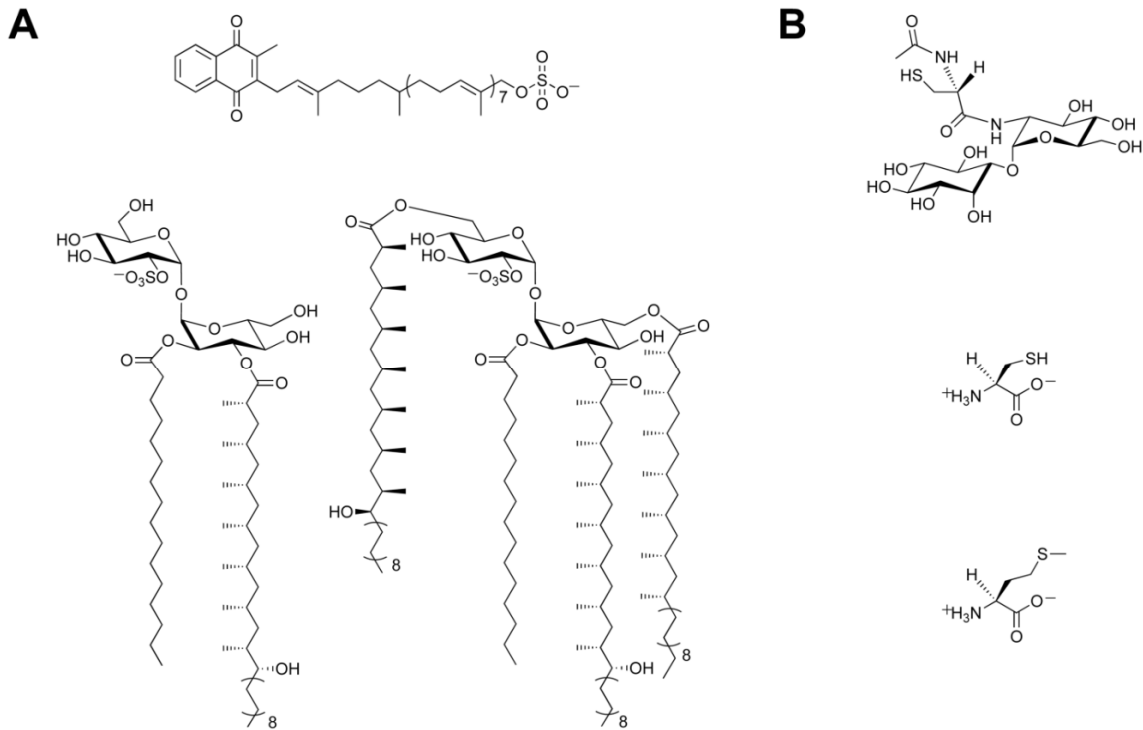


FIGURE 1-1. Sulfur-containing metabolites in *Mtb*. A) Sulfated metabolites, clockwise from top: S881, Sulfolipid-1, and SL₁₂₇₈. B) Reduced sulfur metabolites, from top to bottom: mycothiol (MSH), cysteine, and methionine.

There is a growing body of evidence that implicate the importance of sulfur-containing metabolites in *Mtb* pathogenesis [8, 9], and sulfated molecules have been correlated with virulence (**Figure 1-1A**) [10-12]. In particular, an abundant cell-wall associated sulfated glycolipid, sulfolipid-1 (SL-1), which constitutes approximately 1% of the dried weight of *Mtb*, is uniquely present in pathogenic *Mtb* complex [10, 13]. The strain virulence has been positively correlated with the amounts of SL-1 [14]. Both SL-1 and its precursor SL₁₂₇₈, named based on its observed mass, are capable to elicit cytokine production in TB patients [12]. However, the sulfated menaquinone S881 has been shown to suppress virulence [11]. On the other hand, the reduced sulfur metabolites, such as cysteine and methionine (**Figure 1-1B**) also contribute to *Mtb* pathogenesis [8]. In mouse infection model, *Mtb* mutants defective in the production of reduced sulfur compounds exhibit attenuated virulence during the chronic phase of infection [15]. Mycothiol (MSH), the most abundant sulfhydryl-containing molecule in Mycobacteria, provides protection against oxidative stress and detoxification of bactericidal agents [16-18]. The biosynthesis of the aforementioned sulfur-containing metabolites depends upon the sulfate assimilation pathway [19].

The sulfate assimilation pathway in *Mtb*

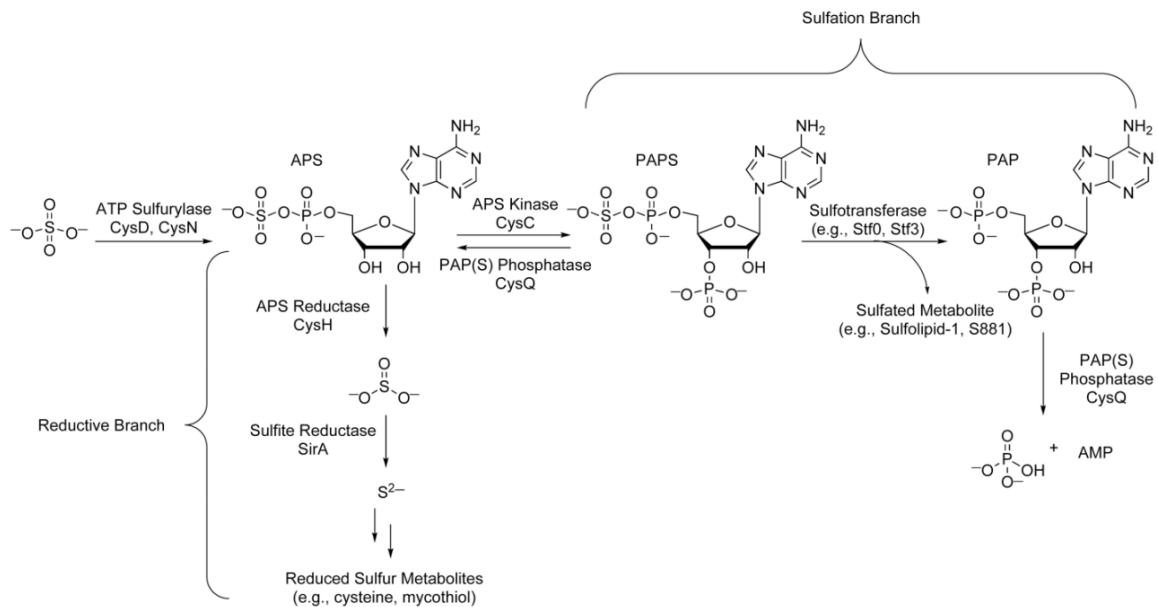


FIGURE 1-2. The sulfate assimilation pathway of *Mtb*. After being actively transported into the cytoplasm, the inorganic sulfate is chemically activated to form APS by ATP sulfurylase. APS can either proceed through the reductive branch or the sulfation branch of the pathway. In the reductive branch, APS is reduced by APS reductase to form sulfite, which is then further reduced by sulfite reductase for the biosynthesis of essential reduced sulfur metabolites. Alternatively, in the sulfation branch, APS is phosphorylated by APS kinase to form PAPS, which is a universal sulfate donor of the cell catalyzed the enzyme sulfotransferases. The byproduct of the reaction, PAP is dephosphorylated by PAP(S) phosphatase CysQ, which also recycles APS from PAPS

The sulfate assimilation pathway (**Figure 1-2**) initiates with the active transport of extracellular inorganic sulfate into the cell [9]. Once in the cytoplasm, the sulfate molecule is then activated by adenylation by ATP sulfurylase (CysD) to produce adenosine 5'-phosphosulfate (APS). The formation of the high energy phosphoric-sulfuric acid anhydride bond couples the hydrolysis of GTP by the GTPase (CysN), effectively compensates for the unfavorable reaction [20]. Through the reductive branch of the pathway, APS is subsequently reduced to sulfite by APS reductase (CysH) then further reduced to sulfide by sulfite reductase (SirA), and ultimately incorporated for the biosynthesis of reduced sulfur metabolites [21]. Alternatively, via the sulfation branch of the pathway, APS is phosphorylated by APS kinase at the 3'-position to form 3'-phosphoadenosine 5'-phosphosulfate (PAPS), which is the universal sulfate donor in the cell [19]. Sulfotransferases is a class of enzymes that catalyze the transfer of the sulfate group on PAPS onto other bacterial metabolites [13]. As a means to counteract the product inhibition of PAP on at least one sulfotransferases in Mycobacteria, PAP(S) phosphatase (CysQ) breaks down PAP by dephosphorylation to form AMP and inorganic phosphate. In addition, PAP(S) phosphatase can also recycle APS from PAPS [22]. Together, these genes constitute the sulfation branch of the sulfate assimilation pathway.

There are many environmental cues that influence the expression of the sulfate assimilation pathway. Indeed, during infection *Mtb* encounters constant changes in nutrient concentration, oxygen levels, pH [23-25]. The disruption of *Mtb*'s response to host defenses is an attractive option for searching for potential drug targets. In this chapter, the signals that elicit changes in the sulfate assimilation pathway are discussed to facilitate our understanding of mechanisms that govern bacterial adaptation to the host. The knowledge can further aid us in the discovery of novel therapeutics for tuberculosis.

Regulation of sulfur metabolism genes in facilitating bacterial adaptation

During infection, *Mtb* encounters of myriad of environmental changes as the bacterium proceeds through the life cycle (**Scheme 1-1**). The most dramatic transformation commences after the phagocytosis by a macrophage [8]. *Mtb* is immediately exposed to hostile conditions include oxidative stress and deprivation of essential nutrients and oxygen [20, 23, 26-33].

Microarray analysis has shown that these conditions upregulate key genes in the sulfate assimilation pathway [20, 27, 30, 31]. More specifically, treatment with hydrogen peroxide induces genes that are responsible for the active transport of sulfate (*cysT*) as well as the chemical activation of sulfate (ATP sulfurylase, *cysD*, *cysNC*) (**Figure 1-2**) [20, 27]. Starved *Mtb* cultures also show increase production of *cysD*, *cysNC*, *cysT*, and the gene for PAP(S) phosphatase (*cysQ*) [30, 31]. Moreover, *cysD*, *cysNC*, and genes contributing to the biosynthesis of reduced sulfur metabolites, *cysK2* and *cysM*, are induced by hypoxia. These genes regulate the first steps of the sulfate assimilation pathway, and the induction is likely accompanied by the increase in the biosynthesis of sulfur-containing metabolites. Notably, during macrophage infection, *CysD* and *CysNC* are also induced, highlighting the essentiality of sulfur metabolism to intracellular survival [27, 29]. The finding is corroborated with the discovery that reduced sulfur metabolites play a critical role in facilitating bacterial persistence in TB mouse infection

model [15]. Together, these reports suggest genes responsible for sulfur metabolism are likely to facilitate bacterial adaptation to the harsh microenvironment in the phagosomes, and the inhibition of this pathway may be an attractive anti-tuberculosis therapy.

Small molecule inhibition of enzymes in the sulfate assimilation pathway

Sulfation Branch

Sulfotransferases are one of the most investigated genes in the sulfate assimilation pathway, particularly due to the abundance of sulfated molecules in eukaryotic organisms. In mammals, they function primarily in mediating cell-cell communications [11]. Among all pathogenic bacteria, only one family, the Mycobacteria, produce sulfated metabolites, and its function is thought to facilitate host-pathogen interactions [34]. In *Mtb* there are four genes identified as sulfotransferases, based on sequence similarity to eukaryotic homologs (annotated as *stf0-3*) [9], and their roles in virulence was investigated. A knockout mutant of *stf0* exhibits non-essentiality in liquid culture, which suggests a specific unknown role in host infection [35]. In a related study, *stf3* knockout displayed a hypervirulent phenotype in a mouse model of TB infection [11]. Although the roles of sulfated metabolites in the *Mtb* lifecycle are still under investigation, the use of small molecule inhibitors of sulfotransferases may assist in uncovering their respective substrates.

Armstrong and coworkers used a kinase-directed library to search for small molecule inhibitors of the bacterial sulfotransferase NodH from *Rhizobium meliloti* [36, 37]. Since PAPS, the substrate for sulfotransferases, shares the same adenosine moiety as ATP, the cross-reactivity can be exploited. Of the 139 compounds screened, the 6 most potent compounds have moderate potency with half maximal inhibitory concentrations (IC_{50}) between 20 μ M and 40 μ M.

Screening for sulfotransferases is a promising start in drug discovery efforts, but to date, sulfotransferase inhibitors lack potency and specificity. Recent advances in high-throughput screening (HTS) should greatly facilitate the discovery of new sulfotransferase inhibitors.

Reductive Branch

The reductive branch of the sulfate assimilation pathway has been shown to be critical for bacterial persistence during the chronic stage of infection in mice, and the reduced sulfur metabolites are thought to counter the oxidative stress elicited by host immune cells [8, 9, 15, 38]. Therefore, inhibition of this pathway may be an excellent approach for targeting the latent phase of tuberculosis.

The first committed step of the reductive branch, which is catalyzed by APS reductase, has a 4[Fe-S] cluster near the active site [21]. The cluster is prone to auto-oxidation by air, so is not amendable to conventional high throughput screening. To overcome this limitation, Cosconati and coworkers designed a virtual screening platform based on computational docking methods. Most potent compounds were validated biochemically [39]. Based on structure-activity relations (SAR) from the previous study,

critical ligand binding determinants were identified [40]. This study provides the foundation for further optimization of compounds that specifically inhibit the reductive branch of the sulfate assimilation pathway.

As previously mentioned, the reductive branch has shown to be critical in the maintenance of the persistent phase of infection in mouse TB infection model [15]. Chemical inhibitors of the sulfate assimilation pathway could potentially give rise to drugs that can shorten the duration of chemotherapy and specifically targeting the latent stage of TB infection.

Summary

The identification of novel therapeutics is urgently needed in order to combat increasing drug-resistant and latent TB infections. To this end, the sulfate assimilation pathway presents itself as a promising new candidate for anti-TB therapeutics [9, 13, 19]. Transcription analyses have validated the biosynthetic pathway of many sulfur-containing molecules as antimicrobial targets [41-44]. Moreover, sulfur metabolic pathways are required for the expression of virulence in pathogenic bacteria [15, 45, 46]. In Mycobacteria, mutants in the sulfur metabolism genes exhibit severely reduced virulence and the ability to persist and cause disease [15, 47-52]. Most importantly, most prokaryotic sulfur metabolic pathways are absent in humans, thus eliminating the possibility of cross-reactivity. Small molecule inhibitors of the sulfate assimilation pathway not only may represent a new class of drugs against TB, but also valuable chemical tools to investigate its roles in *Mtb* pathogenesis.

Thesis Overview

The hallmark of *Mtb* infection is the ability to subvert the bactericidal mechanisms of macrophages and induce the formation of the granuloma, where it establishes long-term residence. The underlying mechanism is supported by the metabolic adaptation to its enclosed surroundings and the biosynthesis of molecules that mediate the interaction with a plethora of immune cells. In the subsequent chapters, I will present approaches for identification of small molecule inhibitors for ATP sulfurylase, the first committed step of the sulfate assimilation pathway. Chapter 2 highlights the effort towards high throughput screening, including assay optimization, compound library selection and hit identification. Chapter 3 describes the validation and elucidation of the mode of inhibition, generating a group of lead compounds. In addition, derivatives of the parent compounds were tested for structure activity relation analysis. Chapter 4 presents the *in vivo* activity of the lead compounds against Gram positive and Gram negative pathogens as well as its toxicity profile in mammalian Vero cell line.

References

1. World Health Organization. 2012; Available from: <http://www.who.int/tb/en/>.

2. Zhang, Y., *The magic bullets and tuberculosis drug targets*. Annu Rev Pharmacol Toxicol, 2005. **45**: p. 529-64.
3. Chan, E.D. and M.D. Iseman, *Multidrug-resistant and extensively drug-resistant tuberculosis: a review*. Curr Opin Infect Dis, 2008. **21**(6): p. 587-95.
4. Russell, D.G., *Mycobacterium tuberculosis: Here today, and here tomorrow*. Nature Reviews Molecular Cell Biology, 2001. **2**(8): p. 569-577.
5. Lin, P.L. and J.L. Flynn, *Understanding latent tuberculosis: a moving target*. J Immunol, 2010. **185**(1): p. 15-22.
6. Russell, D.G., *Who puts the tubercle in tuberculosis?* Nat Rev Microbiol, 2007. **5**(1): p. 39-47.
7. Boshoff, H.I. and C.E. Barry, 3rd, *Tuberculosis - metabolism and respiration in the absence of growth*. Nat Rev Microbiol, 2005. **3**(1): p. 70-80.
8. Bhave, D.P., W.B. Muse, 3rd, and K.S. Carroll, *Drug targets in mycobacterial sulfur metabolism*. Infect Disord Drug Targets, 2007. **7**(2): p. 140-58.
9. Schelle, M.W. and C.R. Bertozzi, *Sulfate metabolism in mycobacteria*. Chembiochem, 2006. **7**(10): p. 1516-24.
10. Gangadharam, P.R., M.L. Cohn, and G. Middlebrook, *Infectivity, Pathogenicity and Sulpholipid Fraction of Some Indian and British Strains of Tubercle Bacilli*. Tubercle, 1963. **44**: p. 452-5.
11. Mougous, J.D., et al., *A sulfated metabolite produced by stf3 negatively regulates the virulence of Mycobacterium tuberculosis*. Proc Natl Acad Sci U S A, 2006. **103**(11): p. 4258-63.
12. Gilleron, M., et al., *Diacylated sulfoglycolipids are novel mycobacterial antigens stimulating CD1-restricted T cells during infection with Mycobacterium tuberculosis*. Journal of Experimental Medicine, 2004. **199**(5): p. 649-59.
13. Mougous, J.D., et al., *Sulfotransferases and sulfatases in mycobacteria*. Chem Biol, 2002. **9**(7): p. 767-76.
14. Minnikin, D.E., et al., *The methyl-branched fortifications of Mycobacterium tuberculosis*. Chem Biol, 2002. **9**(5): p. 545-53.
15. Senaratne, R.H., et al., *5'-Adenosinephosphosulphate reductase (CysH) protects Mycobacterium tuberculosis against free radicals during chronic infection phase in mice*. Mol Microbiol, 2006. **59**(6): p. 1744-53.

16. Buchmeier, N.A., et al., *Association of mycothiol with protection of Mycobacterium tuberculosis from toxic oxidants and antibiotics*. Mol Microbiol, 2003. **47**(6): p. 1723-32.
17. Jothivasan, V.K. and C.J. Hamilton, *Mycothiol: synthesis, biosynthesis and biological functions of the major low molecular weight thiol in actinomycetes*. Nat Prod Rep, 2008. **25**(6): p. 1091-117.
18. Rawat, M., et al., *Comparative analysis of mutants in the mycothiol biosynthesis pathway in Mycobacterium smegmatis*. Biochem Biophys Res Commun, 2007. **363**(1): p. 71-6.
19. Williams, S.J., et al., *5'-adenosinephosphosulfate lies at a metabolic branch point in mycobacteria*. J Biol Chem, 2002. **277**(36): p. 32606-15.
20. Pinto, R., et al., *The Mycobacterium tuberculosis cysD and cysNC genes form a stress-induced operon that encodes a tri-functional sulfate-activating complex*. Microbiology, 2004. **150**(Pt 6): p. 1681-6.
21. Carroll, K.S., et al., *A conserved mechanism for sulfonucleotide reduction*. PLoS Biol, 2005. **3**(8): p. e250.
22. Hatzios, S.K., A.T. Iavarone, and C.R. Bertozzi, *Rv2131c from Mycobacterium tuberculosis is a CysQ 3'-phosphoadenosine-5'-phosphatase*. Biochemistry, 2008. **47**(21): p. 5823-31.
23. Rustad, T.R., et al., *The enduring hypoxic response of Mycobacterium tuberculosis*. PLoS One, 2008. **3**(1): p. e1502.
24. Abramovitch, R.B., et al., *aprABC: a Mycobacterium tuberculosis complex-specific locus that modulates pH-driven adaptation to the macrophage phagosome*. Mol Microbiol, 2011. **80**(3): p. 678-94.
25. Koo, M.S., S. Subbian, and G. Kaplan, *Strain specific transcriptional response in Mycobacterium tuberculosis infected macrophages*. Cell Commun Signal, 2012. **10**(1): p. 2.
26. Boshoff, H.I., et al., *The transcriptional responses of Mycobacterium tuberculosis to inhibitors of metabolism: novel insights into drug mechanisms of action*. J Biol Chem, 2004. **279**(38): p. 40174-84.
27. Schnappinger, D., et al., *Transcriptional Adaptation of Mycobacterium tuberculosis within Macrophages: Insights into the Phagosomal Environment*. Journal of Experimental Medicine, 2003. **198**(5): p. 693-704.

28. Voskuil, M.I., K.C. Visconti, and G.K. Schoolnik, *Mycobacterium tuberculosis gene expression during adaptation to stationary phase and low-oxygen dormancy*. Tuberculosis (Edinb), 2004. **84**(3-4): p. 218-27.
29. Fontan, P., et al., *Global transcriptional profile of Mycobacterium tuberculosis during THP-1 human macrophage infection*. Infection and Immunity, 2008. **76**(2): p. 717-25.
30. Hampshire, T., et al., *Stationary phase gene expression of Mycobacterium tuberculosis following a progressive nutrient depletion: a model for persistent organisms?* Tuberculosis (Edinb), 2004. **84**(3-4): p. 228-38.
31. Betts, J.C., et al., *Evaluation of a nutrient starvation model of Mycobacterium tuberculosis persistence by gene and protein expression profiling*. Mol Microbiol, 2002. **43**(3): p. 717-31.
32. Manganeli, R., et al., *The Mycobacterium tuberculosis ECF sigma factor sigmaE: role in global gene expression and survival in macrophages*. Mol Microbiol, 2001. **41**(2): p. 423-37.
33. Provvedi, R., et al., *Global transcriptional response to vancomycin in Mycobacterium tuberculosis*. Microbiology, 2009. **155**(Pt 4): p. 1093-102.
34. Daffe, M. and P. Draper, *The envelope layers of mycobacteria with reference to their pathogenicity*. Adv Microb Physiol, 1998. **39**: p. 131-203.
35. Mougous, J.D., et al., *Identification, function and structure of the mycobacterial sulfotransferase that initiates sulfolipid-1 biosynthesis*. Nat Struct Mol Biol, 2004. **11**(8): p. 721-9.
36. Armstrong, J.I., et al., *A library approach to the generation of bisubstrate analogue sulfotransferase inhibitors*. Org Lett, 2001. **3**(17): p. 2657-60.
37. Armstrong, J.I., et al., *Discovery of Carbohydrate Sulfotransferase Inhibitors from a Kinase-Directed Library We thank Sharon Long and Dave Keating for providing both the NodH sulfotransferase and APS Kinase during our preliminary experiments and Jack Kirsch for numerous helpful conversations. J.I.A. and K.G.B were supported by NIH Molecular Biophysics Training Grant (No. T32GM0895). This research was funded by grants to C.R.B. from the Pew Scholars Program, the W. M. Keck Foundation and the American Cancer Society (Grant No. RPG9700501BE)*. Angew Chem Int Ed Engl, 2000. **39**(7): p. 1303-1306.
38. Hatzios, S.K. and C.R. Bertozzi, *The regulation of sulfur metabolism in Mycobacterium tuberculosis*. PLoS Pathog, 2011. **7**(7): p. e1002036.

39. Cosconati, S., et al., *Structure-Based Virtual Screening and Biological Evaluation of Mycobacterium tuberculosis Adenosine 5'-Phosphosulfate Reductase Inhibitors*. Journal of Medicinal Chemistry, 2008. **51**(21): p. 6627-6630.
40. Hong, J.A., D.P. Bhave, and K.S. Carroll, *Identification of critical ligand binding determinants in Mycobacterium tuberculosis adenosine-5'-phosphosulfate reductase*. J Med Chem, 2009. **52**(17): p. 5485-95.
41. Aoki, Y., et al., *A new methionine antagonist that has antifungal activity: mode of action*. J Antibiot (Tokyo), 1994. **47**(8): p. 909-16.
42. Ejim, L.J., et al., *Inhibitors of bacterial cystathionine beta-lyase: leads for new antimicrobial agents and probes of enzyme structure and function*. J Med Chem, 2007. **50**(4): p. 755-64.
43. Jacques, S.L., et al., *Enzyme-assisted suicide: molecular basis for the antifungal activity of 5-hydroxy-4-oxonorvaline by potent inhibition of homoserine dehydrogenase*. Chem Biol, 2003. **10**(10): p. 989-95.
44. Kugler, M., et al., *Rhizoctin A, an antifungal phosphono-oligopeptide of Bacillus subtilis ATCC 6633: biological properties*. Arch Microbiol, 1990. **153**(3): p. 276-81.
45. Bogdan, J.A., et al., *Bordetella pertussis autoregulates pertussis toxin production through the metabolism of cysteine*. Infection and Immunity, 2001. **69**(11): p. 6823-30.
46. Lestrade, P., et al., *Identification and characterization of in vivo attenuated mutants of Brucella melitensis*. Mol Microbiol, 2000. **38**(3): p. 543-51.
47. Sassetti, C.M., D.H. Boyd, and E.J. Rubin, *Comprehensive identification of conditionally essential genes in mycobacteria*. Proc Natl Acad Sci U S A, 2001. **98**(22): p. 12712-7.
48. Sassetti, C.M. and E.J. Rubin, *Genetic requirements for mycobacterial survival during infection*. Proc Natl Acad Sci U S A, 2003. **100**(22): p. 12989-94.
49. Sareen, D., et al., *Mycothiols are essential for growth of Mycobacterium tuberculosis Erdman*. J Bacteriol, 2003. **185**(22): p. 6736-40.
50. Huet, G., et al., *Protein splicing of SufB is crucial for the functionality of the Mycobacterium tuberculosis SUF machinery*. J Bacteriol, 2006. **188**(9): p. 3412-4.
51. Huet, G., M. Daffe, and I. Saves, *Identification of the Mycobacterium tuberculosis SUF machinery as the exclusive mycobacterial system of [Fe-S] cluster assembly*:

evidence for its implication in the pathogen's survival. J Bacteriol, 2005. 187(17): p. 6137-46.

52. Buchmeier, N. and R.C. Fahey, *The mshA gene encoding the glycosyltransferase of mycothiol biosynthesis is essential in Mycobacterium tuberculosis Erdman. FEMS Microbiol Lett, 2006. 264(1): p. 74-9.*

Chapter 2: High throughput screening of small molecule inhibitors of *Mtb* ATP sulfurylase

Introduction

Mycobacterium tuberculosis (*Mtb*), the causative agent of tuberculosis (TB) is the world's single most deadly human pathogen and poses a grave threat to global health. An estimated 3 billion, or one-third of the world's population is infected with *Mtb*, and 2 million die each year as a result of the disease [1]. The difficulties in treating infections are stemmed from the requirement of multiple drugs administered over 6 to 9 months [2], the emergence of multidrug-resistant strains [3], and unique feature of the disease progression within human hosts. Infection begins with the entry of *Mtb* into the lungs and phagocytosis by resident alveolar macrophages [4]. Once therein, *Mtb* disrupts the normal maturation of phagosomes into phagolysosomes, inhibits the acidification and activation of lytic enzymes, and replicates within the altered phagosomal compartment [5]. The host responds by recruitment of leukocytes that surround and seclude the infected macrophages in a structure called a granuloma [6]. The confined microenvironment that is deprived of nutrients and oxygen induces *Mtb* to transition metabolically to a latent, non-replicating state, which can persist for years or decades [7]. The breakdown of this metastable equilibrium of immune containment (*e.g.*, via reduced immune capacity associated with aging, HIV coinfection, and immunosuppressant treatment, *etc.*) causes reactivation of *Mtb* replication and progression into active infection. Given that the majority of infected individuals harbor latent *Mtb* – a state that is refractory to all known treatments – there is a considerable interest in understanding the molecular mechanisms underlying entry into, survival during, and exit from latency [5]. Enzymes and pathways that are critical for latency may serve as targets for anti-tuberculosis drugs that treat a major patient population whose needs are presently unmet.

There is a growing body of evidence that implicate the importance of sulfur-containing metabolites in *Mtb* pathogenesis [8, 9]. Specifically, genes responsible for their production are upregulated by environmental cues that mimic the microenvironment during latency [10-19]. These hostile conditions include exposure to oxidative stress and deprivation of essential nutrients [20, 21]. Notably, genes encoding the first committed step of *CysD* and *CysNC* (**Figure 2-1**) are upregulated during treatment with hydrogen peroxide, hypoxia, nutrient starvation, as well as macrophage infection, highlighting their importance in intracellular survival. Together, these two genes encode a bifunctional complex consist of ATP sulfurylase (*CysD* and *CysN*) and APS kinase (*CysC*) [12] and serve as the first two committed steps of the sulfate assimilation pathway. Moreover, in mouse infection model, reduced sulfur metabolites were shown to be essential for maintaining persistence *in vivo* [22]. Collectively, the sulfate assimilation pathway is likely to facilitate bacterial adaptation to the phagosomal environment, and the inhibition of this pathway may be an attractive anti-tuberculosis therapy.

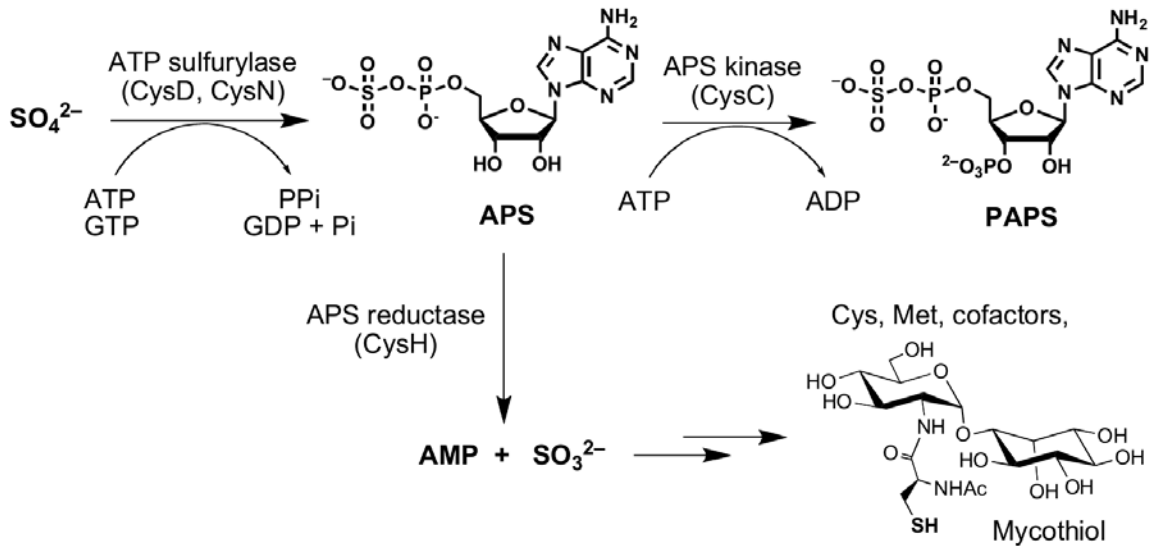


FIGURE 2-1. Sulfate assimilation pathway of *M. tuberculosis*.

The sulfate assimilation pathway (**Figure 2-1**) initiates with the active transport of extracellular inorganic sulfate [9]. Once in the cytoplasm, the sulfate molecule is then activated through adenylation by ATP sulfurylase (*CysD*), together with the hydrolysis of GTP by the GTPase domain (*CysN*), to drive the unfavorable reaction forward [12]. The resulting product, adenosine 5'-phosphosulfate (APS), can be reduced to sulfite by APS reductase (*CysH*) via the reductive branch of the pathway and ultimately for the biosynthesis of reduced sulfur metabolites [23]. Alternatively, APS can be phosphorylated by APS kinase at the 3'-position to form 3'-phosphoadenosine 5'-phosphosulfate (PAPS), which is the universal sulfate donor in the cell [24]. Together, these genes constitute the sulfation branch of the sulfate assimilation pathway.

Small molecule inhibition of the *Mtb* reductive branch had been investigated [25, 26], using virtual screening techniques based on the crystal structure of *Pseudomonas aeruginosa* APS reductase [27]. Indeed, the protein contains an [4Fe-4S] cluster that is air-sensitive and is not amenable to conventional high-throughput screening. However, ATP sulfurylase, which catalyzes the reaction upstream from APS reductase, can potentially provide a means to inactivate reductive branch via small molecule inhibition. ATPS complex consist of two nucleotide (ATP and GTP) binding domains. Curiously, eukaryotic ATPS does not couple APS synthesis with GTP hydrolysis and shares no sequence or structural similarity to the prokaryotic homologs [9]. Given nucleotide binding sites have been subjected to small molecule inhibition, [28] we exploited the structural and mechanistic differences to generate specific inhibitors of sulfate activation.

In this chapter, we first describe the efforts in heterologous expression of *Mtb* ATP sulfurylase in *E. coli*. Western blot and mass spectrometry corroborated and confirmed the identity of the *CysNC* and *CysD* subunits. The complex formation pattern was also consistent with previous reports. Next, we present the evaluation of a commercially available luciferase-based assay, Kinase-Glo+ (Promega), for its potential application in high throughput screening of *Mtb* ATP sulfurylase. The results suggest that the assay is compatible with reaction conditions and yields excellent signal-to-noise ratio.

Lastly, 45 hit compounds with greater than 75% inhibition were presented. Taken together, these findings provide a foundation for further investigation of chemical inhibition of the *Mtb* sulfate assimilation pathway by small molecules. With the potential to manipulate sulfation levels in the cell and regulate the biosynthesis of reduced sulfur-containing metabolites, ATP sulfurylase may be an attractive target for latent-TB therapy.

Results and Discussion

Heterologous expression of Mtb ATP sulfurylase

Mtb ATP sulfurylase was expressed in *E. coli* BL21 (DE3) bearing plasmids containing the *cysD* and *cysNC* genes with N-terminal His₆ tags. To ensure the highest purity for high throughput screening, the purification process involved of three steps. The cell lysate was first passed through a nickel affinity column for the enrichment of the target proteins, followed by an anion exchange column. Then, a final gel filtration step was introduced (**Materials and Methods**). The eluted protein's His₆ sequence was confirmed by an anti-His₆ antibody on a western blot (**Figure 2-2**). Electrospray ionization mass spectrometry (**Figure 2-3**) was used to confirm the identity of the purified proteins whose measured masses (CysD, calculated = 36737.83 Da, observed = 36738.02 Da; CysNC, calculated = 69871.60 Da, observed = 69872.3 Da) were in agreement with the predicted molecular weight, further providing confirmation of the protein's identity.

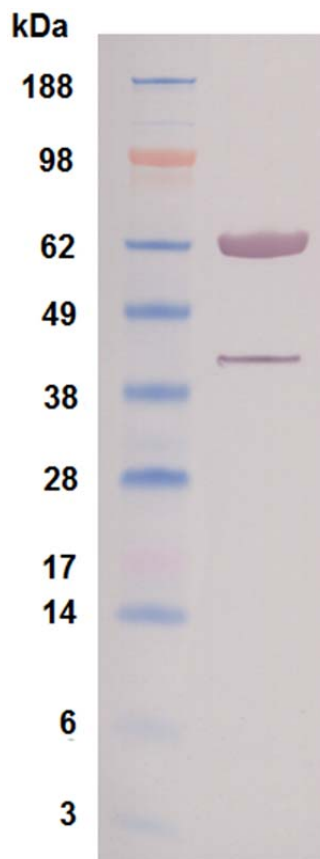


FIGURE 2-2. Western blot analysis detects the presence of two His₆-tagged proteins. The CysNC subunit (calculated: 69.9 kDa) and CysD subunit (calculated: 36.7 kDa) bands are shown near the predicted molecular weight.

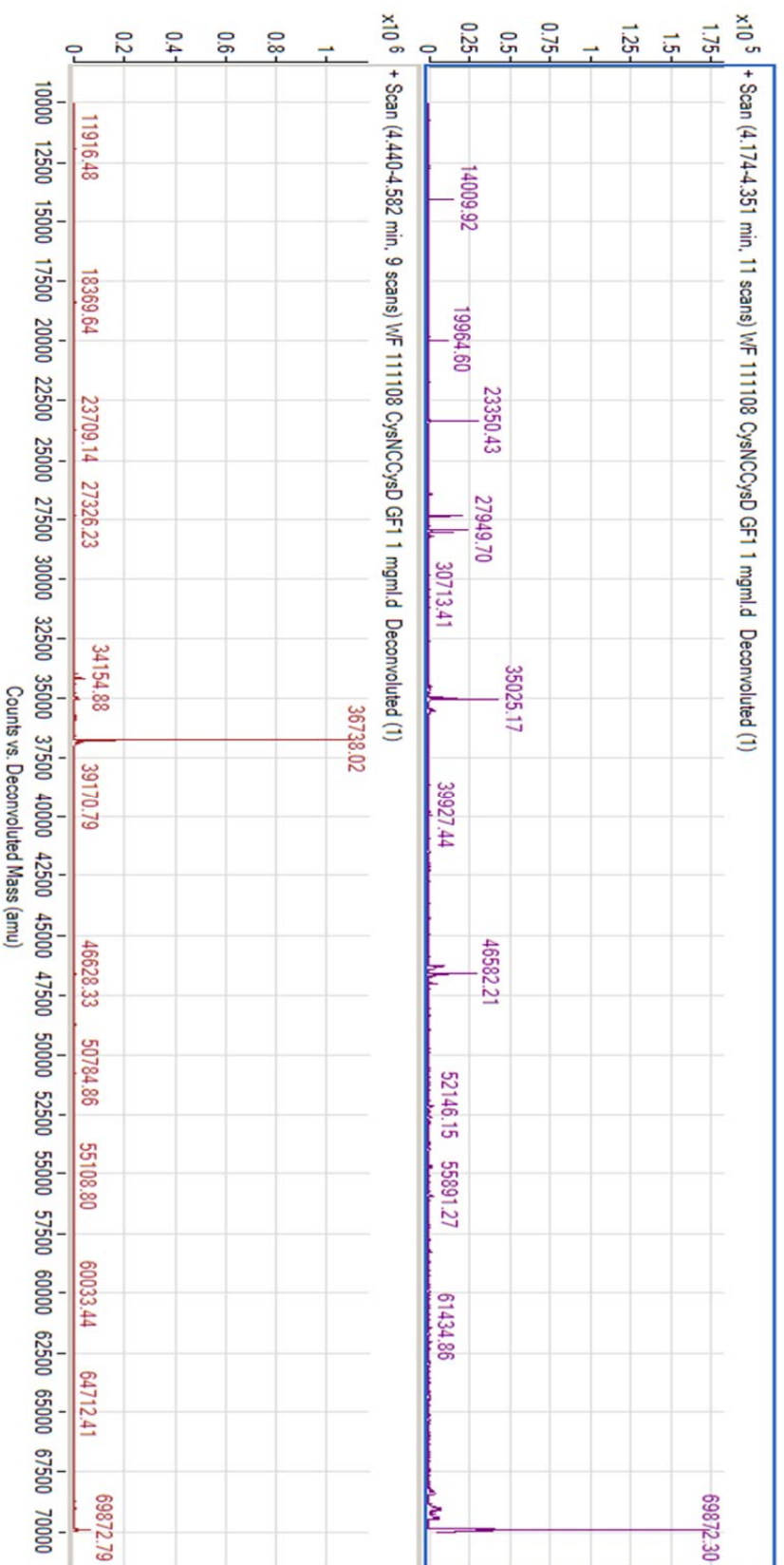


FIGURE 2-3. Mass spectra confirm the identity of the CysNC and CysD subunits (CysD, calculated = 36737.83 Da, observed = 36738.02 Da; CysNC, calculated = 69871.60 Da, observed = 69872.30 Da).

Mtb ATP sulfurylase forms complex oligomers

As previously reported by Leyh and coworkers, *Mtb* ATP sulfurylase forms a sulfate activating complex (SAC) with APS kinase (the N-terminal of the sulfurylation domain, CysN, is fused with APS kinase, CysC). The organization, based on size exclusion chromatography suggest the native quaternary structure consist of a trimer of heterodimers (CysD•CysNC) [29]. By using analytical ultracentrifugation (**Figure 2-4**), the most abundant fraction exists as a hetero hexamer, followed by hetero 12-mer. Hetero 16-mer, 24-mer, and 32-mer are also observed, but in smaller quantities. It should be noted that the complex was exposed to 500 mM NaCl, 10% glycerol, at pH 8 and 15 °C, which may deviate from the natural patterns of complex formation.

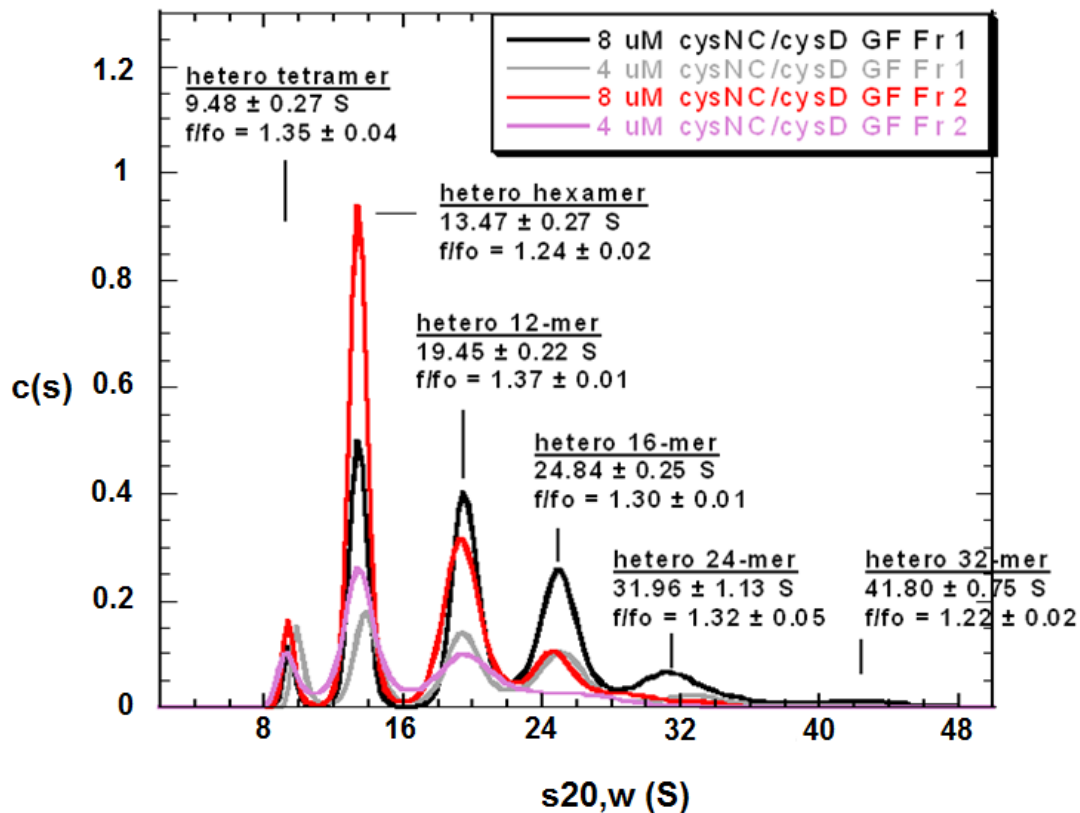


FIGURE 2-4. Analytical centrifugation reveals *Mtb* ATP sulfurylase forms complex oligomers. The most prominent complex corresponds to a hetero hexamer followed by a hetero 12-mer. This result is consistent with finds of Sun *et al.* [29].

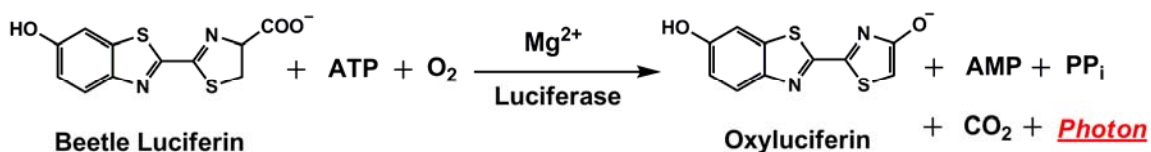
The fusion of APS kinase (CysC) to the GTPase domain of ATP sulfurylase (CysN) raised the interesting possibility of substrate channeling between the two subunits [9, 30]. The channeling hypothesis would implicate that the final product PAPS and not the APS intermediate, would be released into solution. Although PAPS synthesis is 5,800 times more efficient than APS synthesis [29], APS was detected in the solution [30]. The finding that APS is not channeled from the sulfurylation domain (CysD) to the APS

kinase (CysC) domain is consistent with the domain arrangement proposed from a recent structure of the CysNC complex [31].

Since the gene fusion event did not promote substrate channeling, an alternative driving factor might exist. It was shown in *Pseudomonas syringae* ATPS (in *P. syringae*, the C-terminus of CysN is also fused with CysC*, but the kinase activity is abolished by mutations in the ATP binding P-loop. CysC* denotes the inactive domain. There is a second functional copy of CysC, which is located at a different locus in the genome) that when CysC* is truncated, the reaction rate, based on GTP hydrolysis, is reduced 26-fold. In addition, *P. syringae* can no longer form a complex without the CysC domain [31]. This finding suggests complex formation is intimately linked to activity, and it may play a role in modulating the level of PAPS production. Many prokaryotic organisms have evolved intricate transcriptional and translational controls by quorum sensing product concentrations. For example, biosynthesis of the amino acids histidine, phenylalanine, threonine, and tryptophan is controlled by a highly conserved feedback attenuation mechanism [32-36]. It is conceivable that complex formation could serve as an alternative method of regulating the amount of sulfur-containing metabolites. The ability to modulate ATP sulfurylase activity, which governs the production of many sulfur-containing compounds, is critical during infection.

Luciferase-based assay is amenable to high throughput screening

The Kinase-Glo+ reagent (Promega) utilizes the firefly luciferase enzyme, which converts the chemical energy from luciferin oxidation through electron transition, to form oxyluciferin and light (**Scheme 2-1**). The intensity of the luminescence can be positively correlated with ATP concentration with a linear range of 0.1 μM to 100 μM [37]. Due to the modification to the firefly luciferase enzyme, the signal is stable for 4 h and is compatible for use in room temperature. In addition, the buffer contains high concentrations of detergent, such that upon the addition of the reaction mixture, the ATP sulfurylase reaction is quenched.



SCHEME 2-1. Luciferase hydrolyzes ATP to produce luminescence. Using beetle luciferin as a substrate, the luciferase enzyme converts the chemical energy of ATP to photons. The intensity of the luminescence can be positively correlated with ATP concentration.

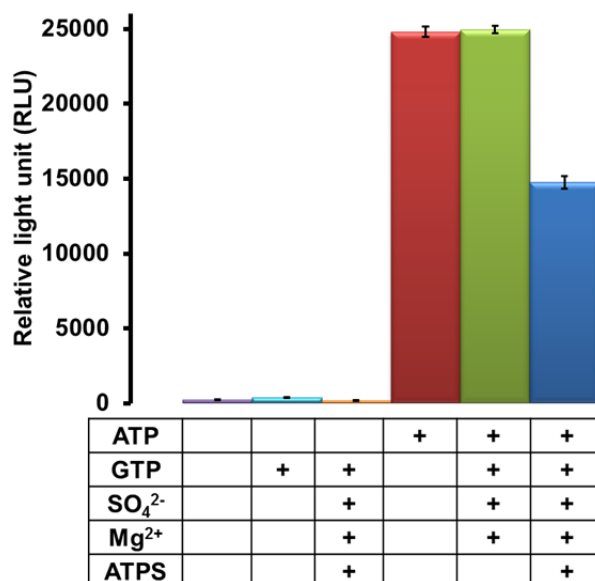


FIGURE 2-5. Luciferase assay is used to assess *Mtb* ATP sulfurylase activity. ATP sulfurylase reaction mixture does not cause interference or artifact in luminescence. Without ATP, Kinase-Glo does not produce luminescence (lanes 1-3), and GTP does not act as an alternative substrate (lane 2). In the presence of ATP, luminescence is observed (lanes 4-6), and GTP does not bind to the ATP site, behaving as a competitive inhibitor (lane 5). With the addition of ATP sulfurylase, there is a decrease in luminescence, indicating the enzyme consumed ATP.

To ascertain whether the ATP sulfurylase reaction mixture can interfere with the luminescence output of the Kinase-Glo+ assay (**Figure 2-5**), the reaction was allowed to proceed without ATP. In lanes 1-3, no luminescence is observed. This is to be expected since ATP is required for luminescence production. The result also eliminated the possibility of firefly luciferase utilizing GTP as an alternative substrate (lane 2). Moreover, ATP sulfurylase did not create background luminescence (lane 3). Next, ATP was added to the reaction mixture (lane 4-6). With only ATP present, the Kinase-Glo+ produced luminescence signal as expected (lane 4). After the addition of GTP, there was no change in luminescence intensity, which suggested that GTP did not act as a competitive inhibitor of firefly luciferase. Lastly, with the addition of ATP sulfurylase, the enzyme consumed ATP, leading to a decrease of luminescence intensity. Taken together, we concluded that the Kinase-Glo+ assay was compatible with the reaction conditions of *Mtb* ATP sulfurylase. The activity of *Mtb* ATP sulfurylase can be measured by determining the amount of ATP consumption, which is correlated with decrease of luminescence signal.

Determining the linear range of Mtb ATP sulfurylase ATP consumption activity

A reaction progress curve was generated to define the linear range of enzyme activity (**Figure 2-6**). Product formation was monitored as a function of time by measuring the luminescence signal generated from the Kinase-Glo+ kit (Promega). The

reaction contained substrate concentrations at the reported K_M of the enzyme [29]. The linear portion of the progression curve was defined to be between 0 and 30 minutes with an R^2 value of 0.9846 (**Figure 2-6, inset**). A reaction time of 30 minutes, which corresponds to approximately 55% of substrate consumption, was used in subsequent assays, as well as for the measurement of compound inhibition during the high throughput screening process.

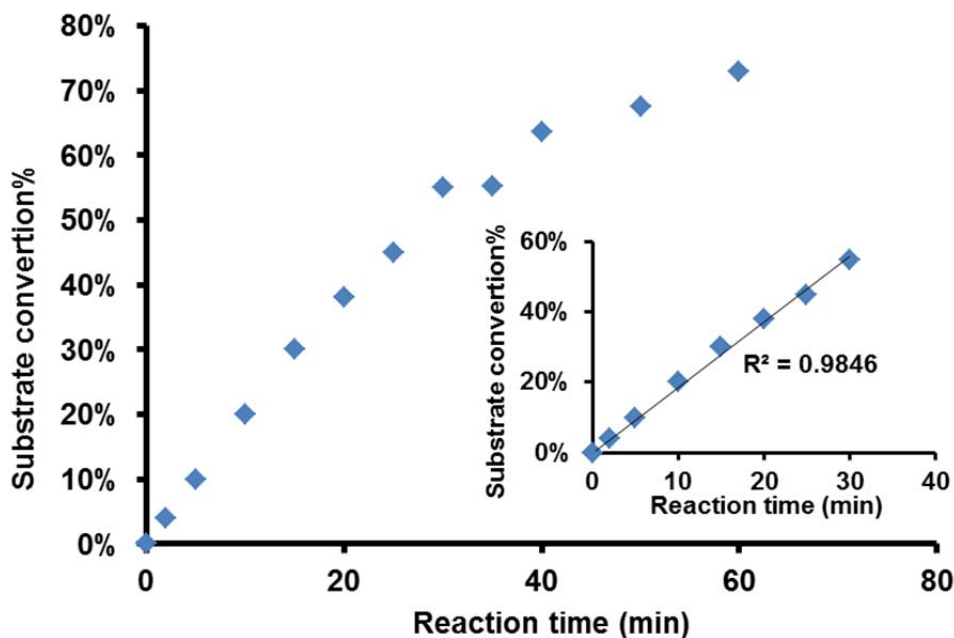


FIGURE 2-6. Reaction progress curve for determining the linear range of *Mtb* ATP sulfurylase. Conditions: 35 μ M ATP, 13 μ M GTP, 1.0 mM Na_2SO_4 , 2.0 mM MgCl_2 , 50 mM HEPES [pH 8.0], 1.2 μ M *Mtb* ATP sulfurylase, at room temperature. The inset shows the linear portion of the curve from 0 to 30 min.

High throughput screen of small molecules inhibitors of the Mtb sulfation pathway

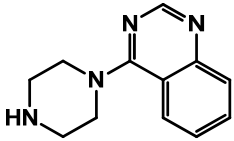
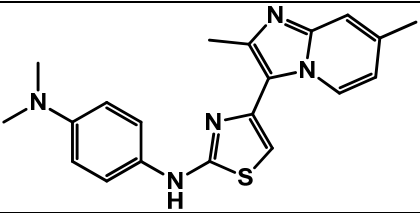
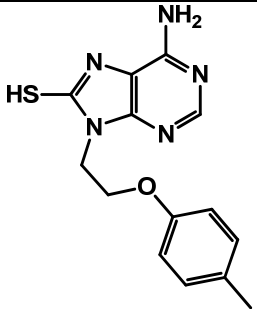
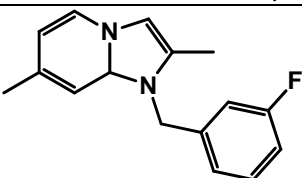
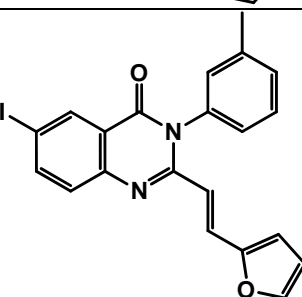
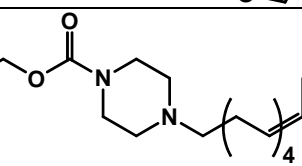
For this study, we pursued three focused library supplied by Small Molecule Discovery Center at University of California, San Francisco (http://smdc.ucsf.edu/documents/documents/CurrentCompounds_2011.pdf). Given *Mtb* ATP sulfurylase contains two nucleotide binding sites, majority of the screened compounds were selected from the Kinase-Targeted Collection. The remaining compounds were derived from the Diversity and Known Bioactive Collections. A total of 9,920 compounds were screened, among them, 7040 compounds were screened from the kinase-targeted collection (22 plates); 1920 compounds were screened from the diversity collection (6 plates); and 960 compounds were screened from the known bioactive collection (3 plates). Small molecules at the concentration of 10 μ M were screened against purified *Mtb* ATP sulfurylase. Enzymatic activity was determined by correlating luminescence with ATP concentrations using Kinase-Glo+ reagent (Promega). A summary of the screening parameters is shown in (**Table 2-1**). Since *Mtb* ATP

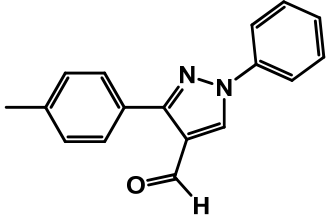
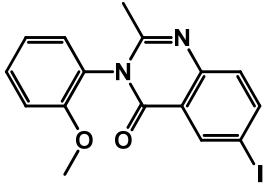
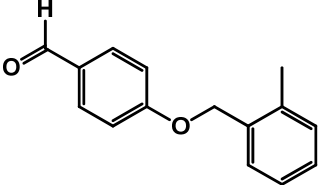
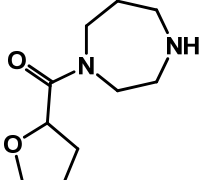
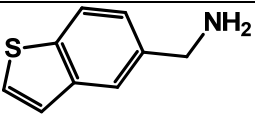
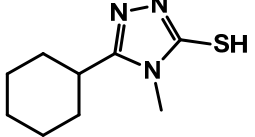
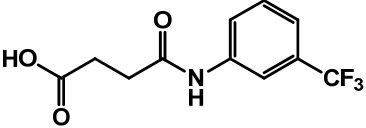
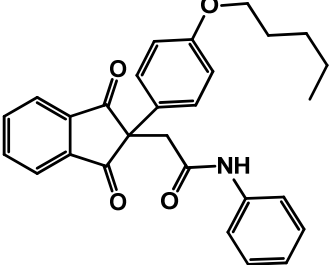
sulfurylase consumes ATP, the absence of ATP consumption, or high luminescence signal, suggest the presence of inhibitory effect on the enzyme. In the scenario that a promiscuous compound inhibits the sulfurylase as well as luciferase enzymes (false negative), the decreased luminescence would suggest high ATP consumption; thus be eliminated from the screen. Setting 75% inhibition as a threshold, the screen identified 45 active compounds (**Table 2-2**). The follow-up secondary screens and validation will be discussed in **Chapter 3**. The quality of the screen was determined by calculating Z factor. For the entire screening process, the Z factor was 0.65 ± 0.05 , which is considered an “excellent” assay [38, 39].

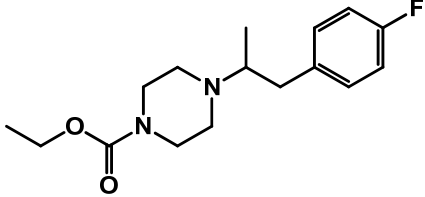
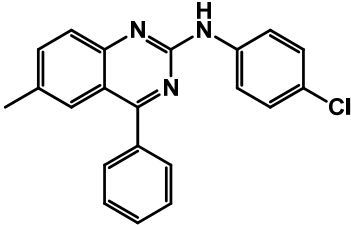
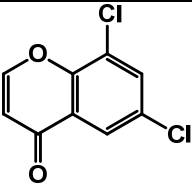
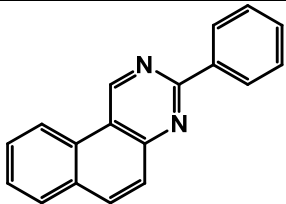
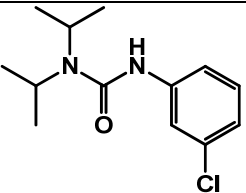
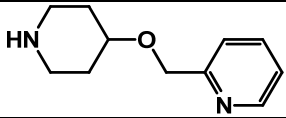
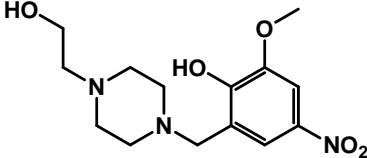
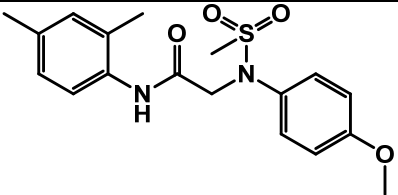
TABLE 2-1. Parameters of the high throughput screening of *Mtb* ATP sulfurylase.

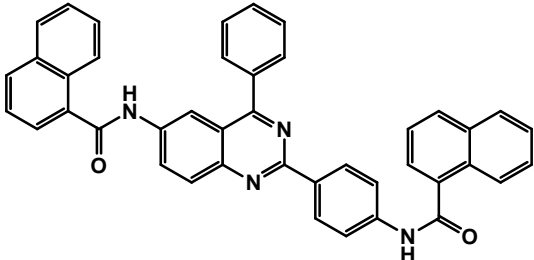
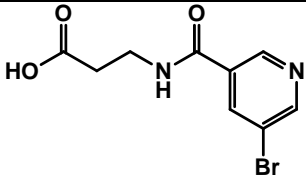
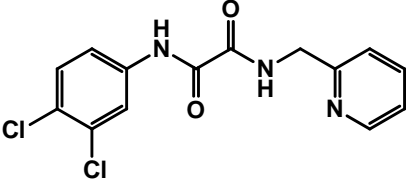
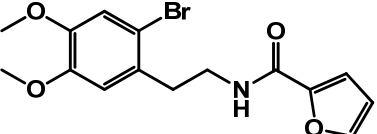
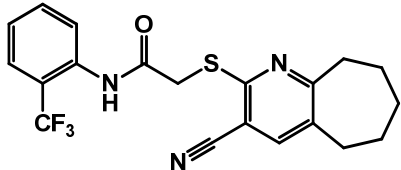
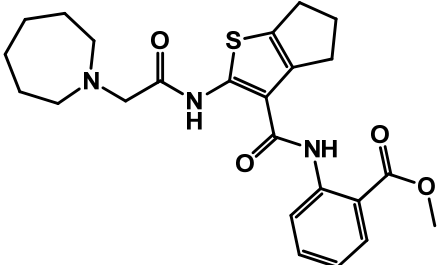
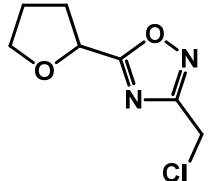
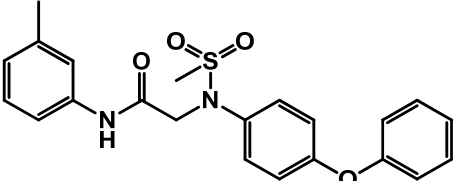
Category	Parameters	Details
Assay	Nature of the assay	Enzymatic assay based on purified <i>Mtb</i> ATP sulfurylase
	Assay strategy	Detection of consumption of ATP
	Reagents and sources	Kinase-Glo+ (Promega)
	Assay protocol	Key steps outlined in Materials and Methods
Library	Nature of the library	Selected from 3 collections: Kinase-Targeted, Diversity, and Known Bioactive Collections
	Size of the library	7040 compounds were screened from the Kinase-Targeted Collection (22 plates); 1920 compounds were screened from the Diversity Collection (6 plates); and 960 compounds were screened from the Known Bioactive Collection (3 plates)
	Source	The kinase-targeted collection came from ChemDiv; the diversity collection came from ChemBridge, and known bioactive collection came from Microsource
	Concentration tested	Constant at 10 μ M concentration at 1% DMSO. 1:100 dilution
HTS process	Format	386-well white plate (Greiner)
	Plate controls	GppNp (Sigma-Aldrich) at 10 mM final concentration was added to positive control wells; no compound was added to negative control wells
	Reagents and compound dispensing systems	Biomek FXp liquid handler (Beckman Coulter) for dispensing compounds and WellMate multichannel dispenser (Matrix) for adding reagents
	Normalization	% inhibition = $100 \times (\text{corrected sample result} - \text{average of positive control}) / (\text{average of negative result} - \text{average of positive control})$
	Performance	Assay performance was determined by the calculation of Z-factor. The Z factor value of 0.65 ± 0.05 is considered to be excellent [38]. (see Material and Methods)

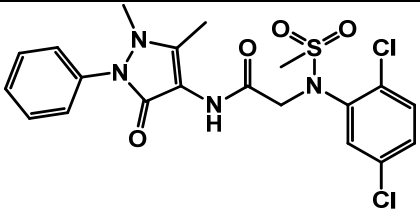
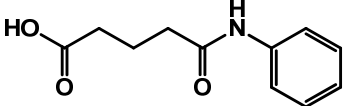
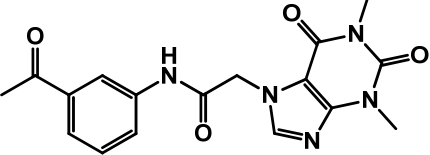
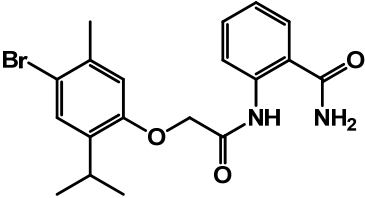
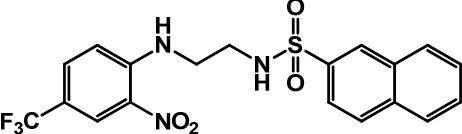
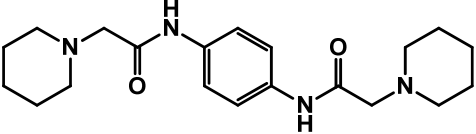
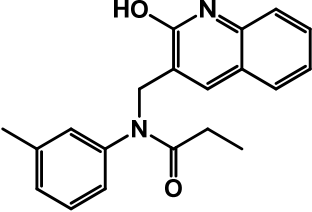
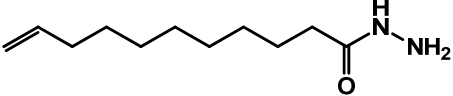
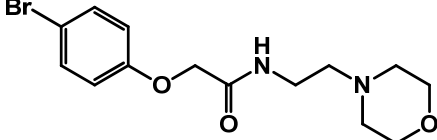
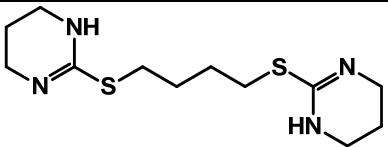
TABLE 2-2. Structures, Lipinski parameters, and percent inhibition of the 45 hit compounds

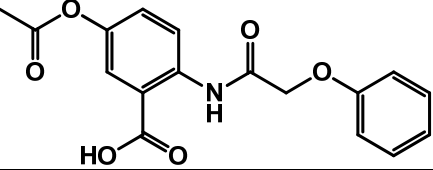
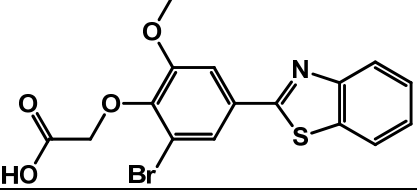
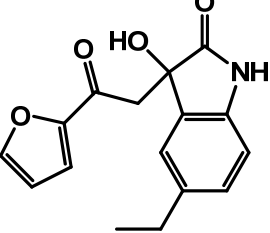
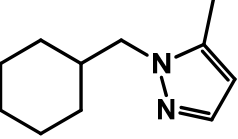
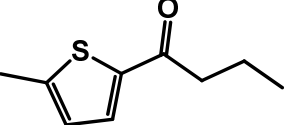
Structure	MW	Log <i>P</i>	H-bond donors / acceptor	Lipinski rule of 5 ^a	Percent inhibition
	214.266 g/mol	1.59	1/4	Satisfied (4/4)	88.0%
	363.479 g/mol	4.25	1/4	Satisfied (4/4)	87.6%
	301.367 g/mol	2.63	2/5	Satisfied (4/4)	86.6%
	256.318 g/mol	3.28	0/2	Satisfied (4/4)	86.6%
	454.260 g/mol	5.52	0/2	One violation (3/4)	86.0%
	324.501 g/mol	4.56	0/2	Satisfied (4/4)	84.9%

	262.306 g/mol	4.32	0/2	Satisfied (4/4)	84.6%
	392.191 g/mol	3.43	0/3	Satisfied (4/4)	83.9%
	246.689 g/mol	3.86	0/2	Satisfied (4/4)	83.7%
	198.262 g/mol	-0.62	1/3	Satisfied (4/4)	83.4%
	199.700 g/mol	1.98	1/1	Satisfied (4/4)	83.0%
	197.301 g/mol	2.13	1/2	Satisfied (4/4)	82.8%
	261.197 g/mol	1.91	2/3	Satisfied (4/4)	82.6%
	441.518 g/mol	5.61	1/4	One violation (3/4)	82.3%

	294.364 g/mol	2.81	0/2	Satisfied (4/4)	81.8%
	345.825 g/mol	6.69	1/3	One violation (3/4)	81.8%
	215.033 g/mol	2.88	0/2	Satisfied (4/4)	81.3%
	256.301 g/mol	4.79	0/2	Satisfied (4/4)	80.4%
	254.756 g/mol	3.48	1/1	Satisfied (4/4)	80.0%
	192.258 g/mol	0.36	1/3	Satisfied (4/4)	79.4%
	311.334 g/mol	-0.54	2/7	Satisfied (4/4)	79.2%
	362.443 g/mol	2.35	1/4	Satisfied (4/4)	79.2%

	620.697 g/mol	9.95	2/4	Two violations (2/4)	79.1%
	273.083	-0.02	2/4	Satisfied	79.0%
	324.162 g/mol	2.38	2/3	Satisfied (4/4)	78.9%
	354.196 g/mol	2.57	1/3	Satisfied (4/4)	78.8%
	405.437 g/mol	5.08	1/3	One violation (3/4)	78.7%
	455.570 g/mol	5.23	2/4	One violation (3/4)	78.6%
	188.612 g/mol	1.41	0/3	Satisfied (4/4)	78.4%
	424.513 g/mol	4.06	1/3	Satisfied (4/4)	78.1%

	483.368 g/mol	1.63	1/5	Satisfied (4/4)	78.0%
	207.226 g/mol	1.48	2/3	Satisfied (4/4)	77.4%
	355.348 g/mol	-0.08	1/5	Satisfied (4/4)	77.3%
	405.286 g/mol	4.76	2/3	Satisfied (4/4)	77.2%
	439.408 g/mol	4.53	2/5	Satisfied (4/4)	77.0%
	358.478 g/mol	1.93	2/4	Satisfied (4/4)	76.9%
	320.385 g/mol	4.46	1/3	Satisfied (4/4)	76.7%
	198.305 g/mol	2.63	2/2	Satisfied (4/4)	76.5%
	343.216 g/mol	1.28	1/4	Satisfied (4/4)	76.2%
	448.284 g/mol	1.80	2/4	Satisfied (4/4)	75.8%

	329.304 g/mol	2.64	2/5	Satisfied (4/4)	75.6%
	394.240 g/mol	3.85	1/5	Satisfied (4/4)	75.5%
	285.295 g/mol	1.92	2/3	Satisfied (4/4)	75.3%
	178.274 g/mol	2.71	0/1	Satisfied (4/4)	75.2%
	168.256 g/mol	3.23	0/1	Satisfied (4/4)	74.6%

^aLipinski rule of 5s [40] states that orally active drugs should possess the following criteria:

- No more than 5 hydrogen bond donors
- No more than 10 hydrogen bond acceptors
- A molecular mass of less than 500 g/mol
- An octanol-water partition coefficient ($\log P$) of less than 5

The Lipinski parameters are listed with the % inhibition, and violations were colored in red.

Conclusions

The emergence of antibiotic resistance fueled by long treatment regimen can be directly attributed to the mycobacterial persistence in *Mtb*. The field of TB drug discovery urgently stresses the need for new target identification to increase the candidates in the pipeline. To that end, mycobacterial sulfur metabolic pathways represent a promising new area for anti-TB therapy. Moreover, since sulfur assimilation pathway is highly conserved among pathogenic bacteria, small molecule inhibitors of this pathway could potentially become a broad spectrum antibiotic.

In this chapter, we present the efforts to establish a high throughput screening program for small molecules that inhibit the activity of *Mtb* ATP sulfurylase. The enzyme was expressed heterologously in *E. coli* and validated with anti-His₆ Western Blot and mass spectrometry. A luciferase- based assay was selected, based on the compatibility to reaction conditions and high Z factor values, to determine the inhibitory effects during the high throughput screen. Of the 9,920 compounds screened, 45 exhibited greater than 75% inhibition. They were subjected to validation and further characterization (**Chapter 3**). These compounds are the first inhibitors of the sulfate assimilation pathway to be reported and potentially have therapeutic applications in the treatment of latent form of TB.

Materials and Methods

Expression and purification of Mtb CysND•CysC in E. coli

pET28b_CysND and pET21a_CysC were co-transformed into *E. coli* strain BL21(DE3). Selected double transformants were used to streak for single colonies. The single colonies were used to inoculate 4-L cultures of LB medium containing 100 mg/L kanamycin and 100 mg/L ampicillin. The cultures were incubated at 37 °C for approximately 4 h with shaking at 250 rpm until an OD₆₀₀ of 0.6 was reached. Protein expression was induced by the addition of isopropyl β-D-thiogalactoside (IPTG) to a final concentration of 100 μM for an additional 16 h at 18 °C. *E. coli* cells were harvested by centrifugation (6000 rpm, 4 °C, 15 min). The pelleted cells were resuspended in 15 ml of lysis buffer (50 mM Tris [pH 7.5], 0.5 M NaCl, 10% glycerol [v/v], 15 mM imidazole, 2 mM β-mercaptoethanol and 1 complete ultra, EDTA-free protease inhibitor cocktail tablet (Roche) at 4 °C. Cells were lysed by ultrasonication (Misonix Sonicator 3000). The cell lysate was cleared by centrifugation (18,500 rpm, 4 °C, 20 min). The resulting supernatant was loaded onto a Ni-NTA column pre-equilibrated with lysis buffer supplemented with 25 mM imidazole. Proteins were washed with lysis buffer supplemented with 100 mM imidazole and subsequently eluted with a gradient of 500 mM imidazole and selected fractions were pooled.

Large-scale expression and purification of Mtb CysND•CysC in E. coli

E. coli strain BL21(DE3) bearing pET28b_CysND and pET21a_CysC plasmids was prepared as described previously. A 1 L overnight culture was prepared from a single colony and used to inoculate 18 L of LB containing 100 mg/L kanamycin and 100 mg/L ampicillin in a C20 fermentor (Sartorius BBI Systems, Inc.). The recombinant protein expression was induced at an OD₆₀₀ of 1.0 by adding IPTG to a final concentration of 0.5 mM. Cells were harvested overnight and frozen at -80 °C prior to purification. Cells were pelleted by centrifugation (37,000 × g, 4 °C, 1 h) and resuspended in lysis buffer (50 mM Tris [pH 8.0], 0.5 M NaCl, 5% glycerol, and 2 mM β-mercaptoethanol). The resulting supernatant was loaded at 5 mL/min onto a Ni-NTA column, which was pre-equilibrated with with buffer A (lysis buffer supplemented with 50 mM imidazole). The column was washed with 10 column volumes (CV) of buffer A, and bound proteins were eluted with

20 CV of imidazole gradient of (50-500 mM) at 5 mL/min and selected fractions were pooled. The pooled fractions were diluted 1:10 [v/v] with Q15 buffer A (25 mM Tris [pH 8.0], 10% glycerol, 1 mM DTT) and loaded onto a anion-exchange column (Source Q15, GE Healthcare) previously equilibrated with Q15 buffer A. Bound protein was eluted with a linear NaCl gradient (30 CV) from 0 to 0.5 M NaCl. Q15 pool was diluted 1:1 [v/v] with butyl Sepharose hydrophobic interaction chromatography (BS-HIC) buffer (25 mM Tris [pH 8.0], 10% glycerol, 1 mM DTT) containing 1.0 M (NH₄)₂SO₄ and loaded onto a butyl Sepharose HIC column (5-mL HiTrap column, GE Healthcare) previously equilibrated with BS-HIC buffer and 0.5 M (NH₄)₂SO₄. Bound protein was eluted with a linear gradient (15 CV) decreasing to 25 mM Tris [pH 8.0], 10% glycerol, 1 mM DTT and fractions were pooled.

Mtb ATP sulfurylase Activity assays

The Kinase-Glo+ reagent (Promega) was used to measure the ATP consumption by *Mtb* ATP sulfurylase. A standard reaction mixture contained 35 μM ATP [$1 \times K_M$], 13 μM GTP [$1 \times K_M$], 1.0 mM Na₂SO₄, 2.0 mM MgCl₂, 1 mM 50 mM HEPES buffer [pH 8.0], 1.2 μM *Mtb* ATP sulfurylase. The reaction was allowed to proceed in room temperature for 30 min and quenched with 1:1 [v/v] of Kinase-Glo+ reagent. In the 96-well format, white, flat-bottom assay plates (Greiner) were used. 50 μL of reaction volume was added with 50 μL Kinase-Glo+ reagent. After a 10 min incubation for Kinase-Glo+ reagent to react and the luminescence signal to equilibrate, the luminescence was determined by a SpectraMax M3 (Molecular Devices). Standard ATP curve was generated by serially diluting 100 μM ATP to 0.78 μM.

High throughput screening

384-well plates containing 320 stock compounds at the concentration of 1 mM dissolved in 100% DMSO were thawed and placed on a WellMate multichannel dispenser (Matrix). 1 μl of the test compounds were added to 384-well white assay plates (Greiner) for a final concentration of 10 μM compound and 1% DMSO. Guanosine 5'-[β,γ-imido]triphosphate (GppNHp, Sigma-Aldrich) and DMSO were added as a positive control (final concentration 10 mM, 1% DMSO), and 1 μl DMSO was added (1% final concentration) as a negative control. 9 μl of screening buffer (final concentration 18 μM ATP [$1/2 \times K_M$], 6.5 μM GTP [$1/2 \times K_M$], 1.0 mM Na₂SO₄, 2.0 mM MgCl₂, 50 mM HEPES [pH 8.0]) was transferred to the assay plates with the robotic dispenser Biomek FXp liquid handler (Beckman Coulter) followed by the addition of 40 μl of *Mtb* ATP sulfurylase (final concentration 1.2 μM). The reactions were performed at room temperature for 30 min and quenched by the addition of 50 μl Kinase-Glo+ (Promega) and placed on a plate shaker for 10 min at room temperature. The ATP-bioluminescence was measured using the AnalystHT plate reader (Molecular Devices). Percent inhibition was calculated for each well as

$$\left(1 - \frac{RLU_x - RLU_-}{RLU_+ - RLU_-}\right) \times 100\%$$

where RLU_x , RLU_+ , RLU_- are Relative Luminescent Units for each well, positive (GppNp), negative (DMSO) controls, respectively. Z factor was used to evaluate the performance of the assay and was calculated as

$$1 - \frac{3(\sigma_p + \sigma_n)}{A_p - A_n}$$

where σ_p , σ_n , A_p , A_n are the standard deviation and mean values of positive and negative controls, respectively.

References

1. World Health Organization. 2012; Available from: <http://www.who.int/tb/en/>.
2. Zhang, Y., *The magic bullets and tuberculosis drug targets*. Annu Rev Pharmacol Toxicol, 2005. **45**: p. 529-64.
3. Chan, E.D. and M.D. Iseman, *Multidrug-resistant and extensively drug-resistant tuberculosis: a review*. Curr Opin Infect Dis, 2008. **21**(6): p. 587-95.
4. Russell, D.G., *Mycobacterium tuberculosis: Here today, and here tomorrow*. Nature Reviews Molecular Cell Biology, 2001. **2**(8): p. 569-577.
5. Lin, P.L. and J.L. Flynn, *Understanding latent tuberculosis: a moving target*. J Immunol, 2010. **185**(1): p. 15-22.
6. Russell, D.G., *Who puts the tubercle in tuberculosis?* Nat Rev Microbiol, 2007. **5**(1): p. 39-47.
7. Boshoff, H.I. and C.E. Barry, 3rd, *Tuberculosis - metabolism and respiration in the absence of growth*. Nat Rev Microbiol, 2005. **3**(1): p. 70-80.
8. Bhave, D.P., W.B. Muse, 3rd, and K.S. Carroll, *Drug targets in mycobacterial sulfur metabolism*. Infect Disord Drug Targets, 2007. **7**(2): p. 140-58.
9. Schelle, M.W. and C.R. Bertozzi, *Sulfate metabolism in mycobacteria*. Chembiochem, 2006. **7**(10): p. 1516-24.
10. Boshoff, H.I., et al., *The transcriptional responses of Mycobacterium tuberculosis to inhibitors of metabolism: novel insights into drug mechanisms of action*. J Biol Chem, 2004. **279**(38): p. 40174-84.
11. Schnappinger, D., et al., *Transcriptional Adaptation of Mycobacterium tuberculosis within Macrophages: Insights into the Phagosomal Environment*. Journal of Experimental Medicine, 2003. **198**(5): p. 693-704.
12. Pinto, R., et al., *The Mycobacterium tuberculosis cysD and cysNC genes form a stress-induced operon that encodes a tri-functional sulfate-activating complex*. Microbiology, 2004. **150**(Pt 6): p. 1681-6.

13. Voskuil, M.I., K.C. Visconti, and G.K. Schoolnik, *Mycobacterium tuberculosis gene expression during adaptation to stationary phase and low-oxygen dormancy*. Tuberculosis (Edinb), 2004. **84**(3-4): p. 218-27.
14. Rustad, T.R., et al., *The enduring hypoxic response of Mycobacterium tuberculosis*. PLoS One, 2008. **3**(1): p. e1502.
15. Fontan, P., et al., *Global transcriptional profile of Mycobacterium tuberculosis during THP-1 human macrophage infection*. Infection and Immunity, 2008. **76**(2): p. 717-25.
16. Hampshire, T., et al., *Stationary phase gene expression of Mycobacterium tuberculosis following a progressive nutrient depletion: a model for persistent organisms?* Tuberculosis (Edinb), 2004. **84**(3-4): p. 228-38.
17. Betts, J.C., et al., *Evaluation of a nutrient starvation model of Mycobacterium tuberculosis persistence by gene and protein expression profiling*. Mol Microbiol, 2002. **43**(3): p. 717-31.
18. Manganelli, R., et al., *The Mycobacterium tuberculosis ECF sigma factor sigmaE: role in global gene expression and survival in macrophages*. Mol Microbiol, 2001. **41**(2): p. 423-37.
19. Provvedi, R., et al., *Global transcriptional response to vancomycin in Mycobacterium tuberculosis*. Microbiology, 2009. **155**(Pt 4): p. 1093-102.
20. Rohde, K., et al., *Mycobacterium tuberculosis and the environment within the phagosome*. Immunol Rev, 2007. **219**: p. 37-54.
21. Appelberg, R., *Macrophage nutritive antimicrobial mechanisms*. J Leukoc Biol, 2006. **79**(6): p. 1117-28.
22. Senaratne, R.H., et al., *5'-Adenosinephosphosulphate reductase (CysH) protects Mycobacterium tuberculosis against free radicals during chronic infection phase in mice*. Mol Microbiol, 2006. **59**(6): p. 1744-53.
23. Carroll, K.S., et al., *A conserved mechanism for sulfonucleotide reduction*. PLoS Biol, 2005. **3**(8): p. e250.
24. Williams, S.J., et al., *5'-adenosinephosphosulfate lies at a metabolic branch point in mycobacteria*. J Biol Chem, 2002. **277**(36): p. 32606-15.
25. Cosconati, S., et al., *Structure-Based Virtual Screening and Biological Evaluation of Mycobacterium tuberculosis Adenosine 5'-Phosphosulfate Reductase Inhibitors*. Journal of Medicinal Chemistry, 2008. **51**(21): p. 6627-6630.

26. Hong, J.A., D.P. Bhave, and K.S. Carroll, *Identification of critical ligand binding determinants in Mycobacterium tuberculosis adenosine-5'-phosphosulfate reductase*. J Med Chem, 2009. **52**(17): p. 5485-95.
27. Chartron, J., et al., *Substrate Recognition, Protein Dynamics, and Iron-Sulfur Cluster in Pseudomonas aeruginosa Adenosine 5'-Phosphosulfate Reductase*. Journal of Molecular Biology, 2006. **364**(2): p. 152-169.
28. Walker, K. and M.F. Olson, *Targeting Ras and Rho GTPases as opportunities for cancer therapeutics*. Curr Opin Genet Dev, 2005. **15**(1): p. 62-8.
29. Sun, M., et al., *The trifunctional sulfate-activating complex (SAC) of Mycobacterium tuberculosis*. J Biol Chem, 2005. **280**(9): p. 7861-6.
30. Sun, M. and T.S. Leyh, *Channeling in sulfate activating complexes*. Biochemistry, 2006. **45**(38): p. 11304-11.
31. Mougous, J.D., et al., *Molecular basis for G protein control of the prokaryotic ATP sulfurylase*. Mol Cell, 2006. **21**(1): p. 109-22.
32. Hopkins, W.G., N.C. Wilson, and D.G. Russell, *Validation of the physical activity instrument for the Life in New Zealand national survey*. Am J Epidemiol, 1991. **133**(1): p. 73-82.
33. Merino, E., P. Babitzke, and C. Yanofsky, *trp RNA-binding attenuation protein (TRAP)-trp leader RNA interactions mediate translational as well as transcriptional regulation of the Bacillus subtilis trp operon*. J Bacteriol, 1995. **177**(22): p. 6362-70.
34. Babitzke, P., D.G. Bear, and C. Yanofsky, *TRAP, the trp RNA-binding attenuation protein of Bacillus subtilis, is a toroid-shaped molecule that binds transcripts containing GAG or UAG repeats separated by two nucleotides*. Proc Natl Acad Sci U S A, 1995. **92**(17): p. 7916-20.
35. Yang, M., et al., *Translation of trpG in Bacillus subtilis is regulated by the trp RNA-binding attenuation protein (TRAP)*. J Bacteriol, 1995. **177**(15): p. 4272-8.
36. Babitzke, P., *Regulation of tryptophan biosynthesis: Trp-ing the TRAP or how Bacillus subtilis reinvented the wheel*. Mol Microbiol, 1997. **26**(1): p. 1-9.
37. Armstrong, D., *Advanced protocols in oxidative stress*. Methods in molecular biology., 2008, New York, NY: Humana Press. <v. 1 >.
38. Zhang, J.H., T.D. Chung, and K.R. Oldenburg, *A Simple Statistical Parameter for Use in Evaluation and Validation of High Throughput Screening Assays*. J Biomol Screen, 1999. **4**(2): p. 67-73.

39. Sui, Y. and Z. Wu, *Alternative statistical parameter for high-throughput screening assay quality assessment*. J Biomol Screen, 2007. **12**(2): p. 229-34.
40. Lipinski, C.A., et al., *Experimental and computational approaches to estimate solubility and permeability in drug discovery and development settings*. Adv Drug Deliv Rev, 2001. **46**(1-3): p. 3-26.

Chapter 3: Validation and characterization of hit compounds that inhibit of *Mtb* ATP sulfurylase

Introduction

Hit compounds derived from library screens are frequently promiscuous inhibitors [1]. In one study, McGovern and his coworkers uncovered kinase inhibitors that not only active against the kinase in question, but other unrelated enzymes as well [2]. This suggests the mechanism of inhibition is not a competitive. By using dynamic light scattering techniques, they observed these “inhibitors” formed aggregates in solutions with diameter ranged from 30 to 400 nm. The formation of the aggregates decreases the effective concentration of the enzyme [3]. To eliminate the possibility of hit compounds’ promiscuous inhibition by aggregate formation, the calculated half maximal inhibitory concentration (IC_{50}) values must not be significantly affected by changes in enzyme concentration [1-4].

After the confirmation that the compounds inhibit in a competitive manner, it is essential to elucidate the binding mode against *Mtb* ATP sulfurylase. To eliminate the possible interference from the kinase domain (CysC), which also has an ATP binding site, the CysC domain is truncated as described in [5]. The truncated *Mtb* ATP sulfurylase has two possible binding sites for the small molecule inhibitors: ATP binding site at the sulfurylation domain (CysD), and GTP binding site at the GTPase domain. Therefore, I have devised an assay that utilizes the fluorescent non-hydrolyzable nucleotides, 2'/3'-O-(N-Methyl-anthraniloyl)-guanosine-5'-[(β,γ)-imido]triphosphate (*mant*-GppNHp) and 5 μ M 2'/3'-O-(N-Methyl-anthraniloyl)-adenosine-5'-[(α,β)-imido] triphosphate (*mant*-ApCpp). *Mant*-nucleotides fluoresce strongly at 448 nm only upon binding [6, 7], and had previously been used to determine binding modes of other small molecule inhibitors that target nucleotide binding pockets (**Figure 3-1**) [8-11].

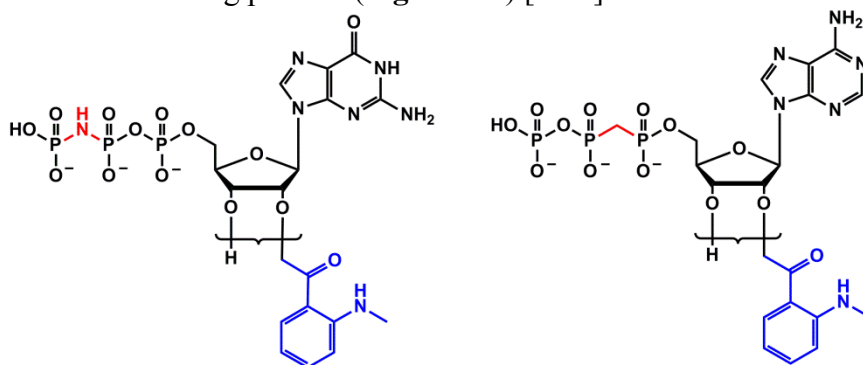
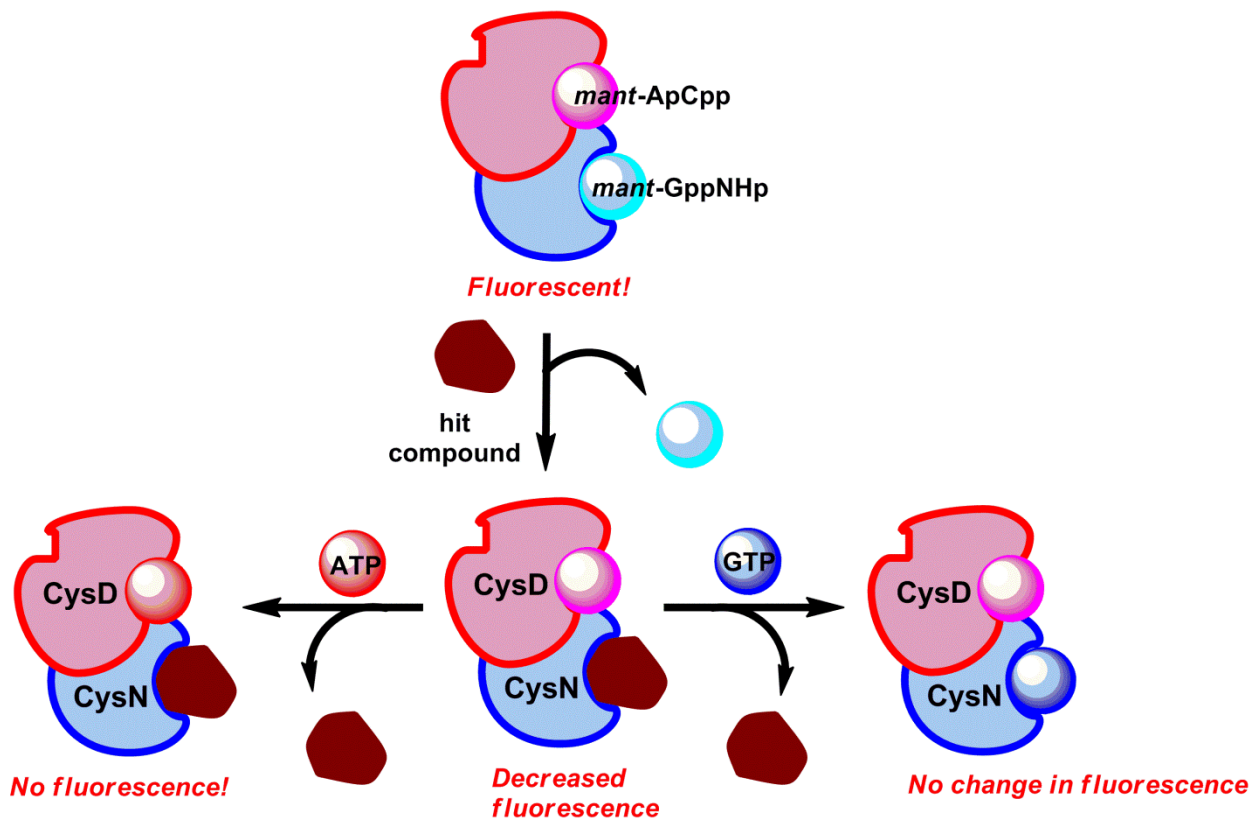


Figure 3-1. Structures of *mant*-GppNHp and *mant*-ApCpp, from left to right. These *mant*-nucleotides fluoresce strongly only upon binding at 448 nm.

The binding assay commences with incubation of *Mtb* ATP sulfurylase with *mant*-GppNHp and *mant*-ApCpp. After equilibrium is achieved, the hit compound in question is added to the reaction mixture. The hit compound competes with one of the *mant*-nucleotides, resulting in a decrease of fluorescence intensity. In the last step,

saturating concentrations of ATP or GTP is added. In the case that the addition of ATP causes a drastic decrease of fluorescence (**Scheme 3-1**, left arrow), this result suggests that the hit compound binds to the G-protein, since ATP outcompetes the fluorescent *mant*-ApCpp. The conclusion can be confirmed by the addition of GTP in the last step, since GTP does not compete with fluorescent *mant*-ApCpp binding, no change in fluorescence will be observed.



SCHEME 3-1. A nucleotide binding pocket competition assay. *Mtb* ATP sulfurylase is first incubated with non-hydrolyzable fluorescent nucleotide analogs *mant*-ApCpp and *mant*-GppNHp. The hit compound is then added to the mixture to compete with the non-hydrolyzable fluorescent analogs – this will result in a decrease of fluorescence. In the next step, either ATP or GTP is added. The nucleotide will out-compete the non-hydrolyzable fluorescent nucleotide, resulting in no fluorescence; or the hit compound, resulting in no change in fluorescence.

In this chapter, the effort towards identifying competitive inhibitors among the 45 hit compounds from the high throughput screen (described in **Chapter 2**) is discussed. All but 6 compounds exhibit propensity to form aggregates with *Mtb* ATP sulfurylase. By using the aforementioned assay to ascertain the binding mechanism, the 6 lead compounds are classified into ATP antagonists and GTP antagonists. One compound in particular, does not occupy either the ATP or GTP site, and is categorized as an allosteric inhibitor [12, 13]. Lastly, by testing the activity of derivative compounds, analysis of structure activity relation is presented. Taken together, this work presents the first

competitive inhibitors of *Mtb* ATP sulfurylase. These compounds have great potential for therapeutic avenue, as well as becoming tools to study the sulfate assimilation pathway via chemical modulation.

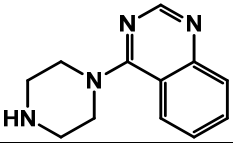
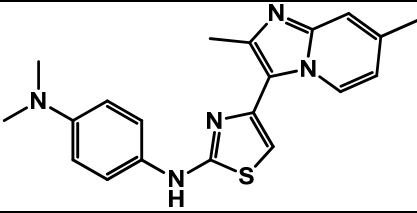
Results and Discussion

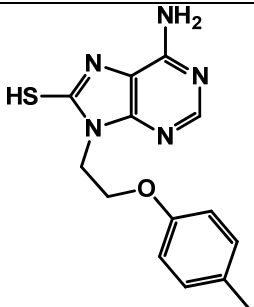
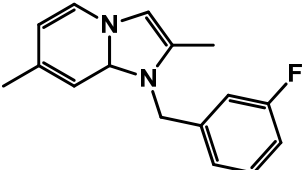
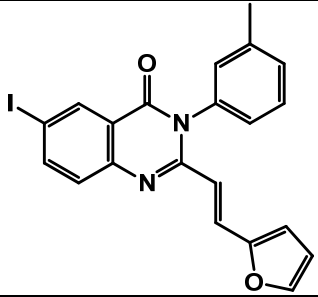
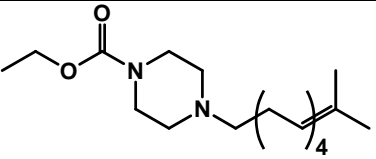
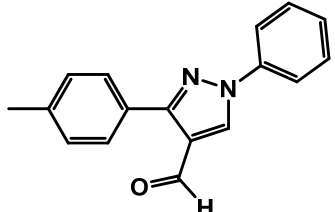
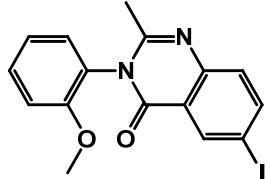
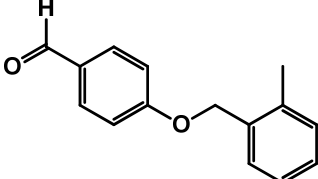
Identification of aggregate forming small molecules among the hit compounds

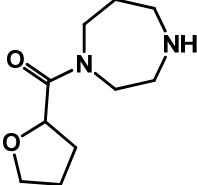
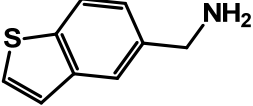
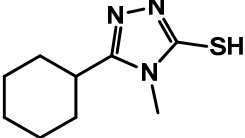
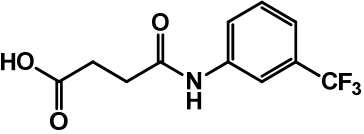
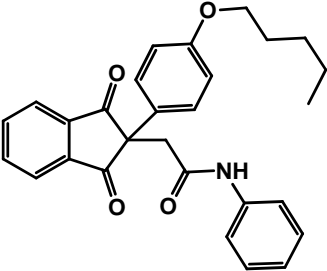
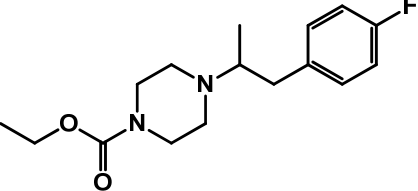
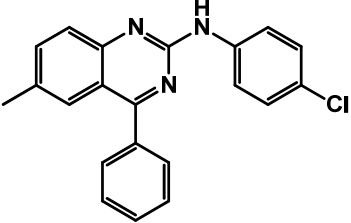
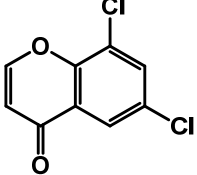
Aggregate-forming compounds are often identified as active inhibitors in high throughput screens [1, 3]. To verify that the compounds were identified by competitive binding, as opposed to forming non-specific aggregates in solution, IC₅₀ values were calculated at two enzyme concentrations, 120 nM and 480 nM (**Table 3-1**). Among the 45 hit compounds from the high throughput screen, 6 compounds that do not form aggregates were boxed.

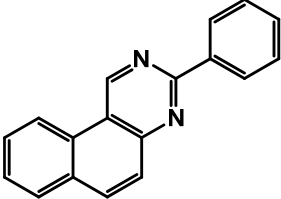
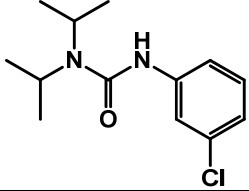
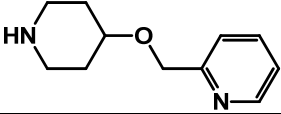
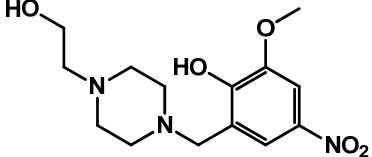
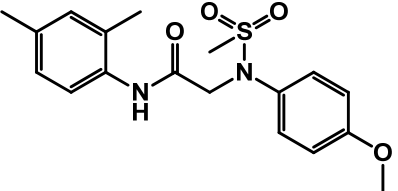
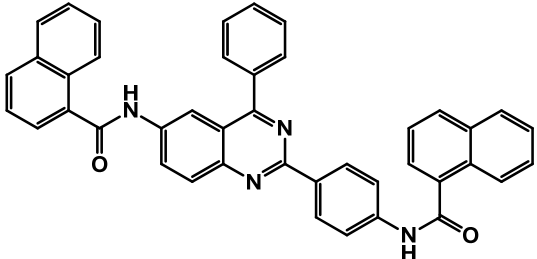
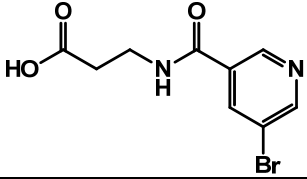
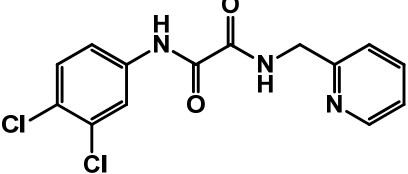
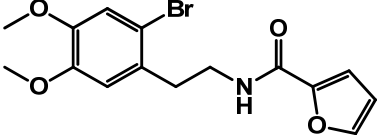
Non-aggregate forming compounds were subjected to a fluorescence assay (**Scheme 1**) to probe the binding site. Briefly, ATP sulfurylase was incubated with non-hydrolyzable fluorescent nucleotide analogs *mant*-ApCpp and *mant*-GppNHp. The hit compound was then added to compete with *mant*-ApCpp or *mant*-GppNHp. This would result in a decrease of fluorescence. In the next step, either ATP or GTP was added and two possible outcomes follow: 1) the nucleotide would out-complete the non-hydrolyzable fluorescent nucleotide, resulting in background fluorescence or 2) the nucleotide would out-compete the hit compound, resulting in no change in fluorescence. To that end, six lead compounds were investigated (**Figure 3-2**). Compounds **1** and **2** were shown to bind in the same site as GTP, and compounds **4**, **5**, and **6** occupied the ATP binding site. Interestingly, compound **3** could not out-complete either *mant*-ApCpp or *mant*-GppNHp. The finding suggests that **3** may inhibit *Mtb* ATPS via allosteric interactions [14]. Data are shown in **Figure 3-3**.

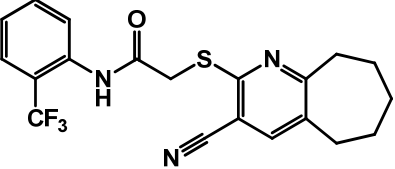
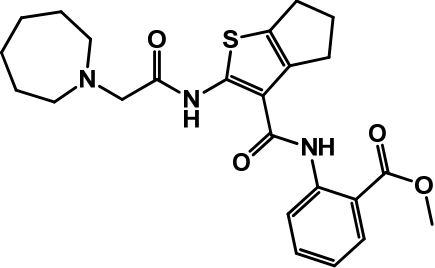
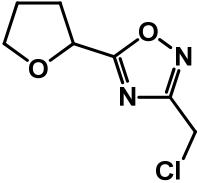
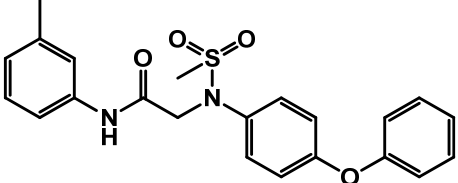
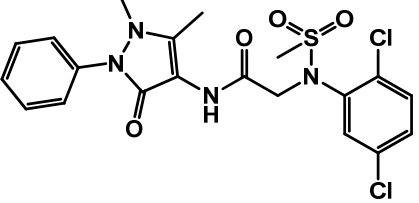
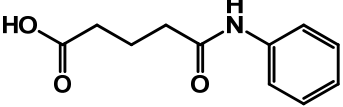
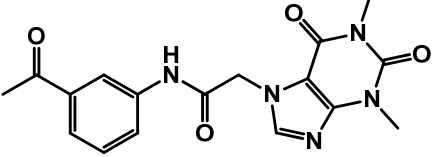
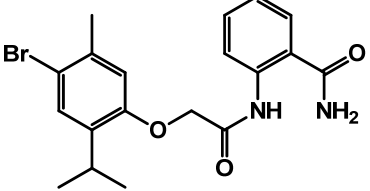
TABLE 3-1. Determination of the aggregate forming propensities of the hit compounds by measuring IC₅₀ values at different enzyme concentrations

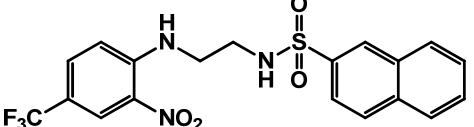
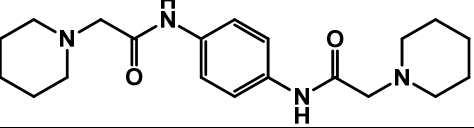
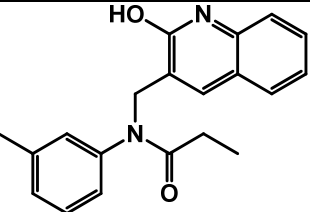
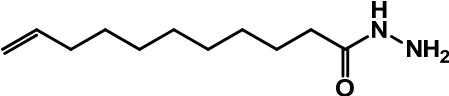
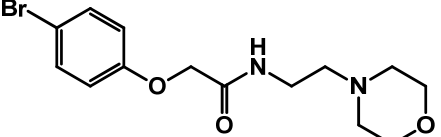
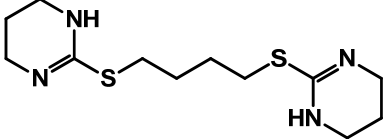
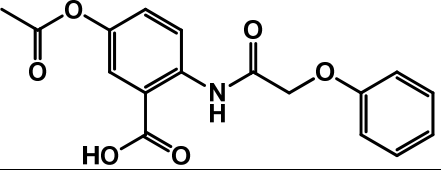
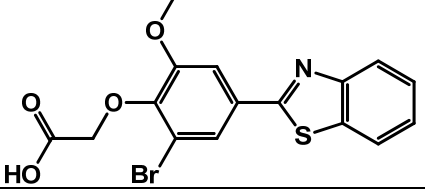
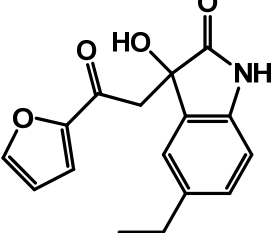
Structure	IC ₅₀ ^a at 120 nM enzyme concentration	IC ₅₀ ^a at 480 nM enzyme concentration	Form aggregate ^b ?
	5.7 ± 1.3 μM	6.1 ± 0.81 μM	no
	7.2 ± 0.9 μM	6.9 ± 1.2 μM	no

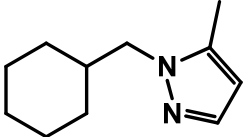
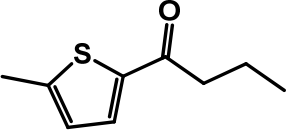
	$57 \pm 9.6 \mu\text{M}$	$53 \pm 9.1 \mu\text{M}$	no
	$6.3 \pm 0.82 \mu\text{M}$	$230 \pm 28 \mu\text{M}$	yes
	$12 \pm 2.2 \mu\text{M}$	$500 \pm 16 \mu\text{M}$	yes
	$8.7 \pm 7.6 \mu\text{M}$	$130 \pm 9.1 \mu\text{M}$	yes
	$11 \pm 2.4 \mu\text{M}$	$71 \pm 11 \mu\text{M}$	yes
	$16 \pm 2.1 \mu\text{M}$	$84 \pm 5.8 \mu\text{M}$	yes
	$96 \pm 12 \mu\text{M}$	$250 \pm 31 \mu\text{M}$	yes

	$140 \pm 18 \mu\text{M}$	$870 \pm 74 \mu\text{M}$	yes
	$32 \pm 1.6 \mu\text{M}$	$140 \pm 4.5 \mu\text{M}$	yes
	$27 \pm 3.7 \mu\text{M}$	$270 \pm 32 \mu\text{M}$	yes
	$21 \pm 3.7 \mu\text{M}$	$89 \pm 6.8 \mu\text{M}$	yes
	$62 \pm 9.1 \mu\text{M}$	$350 \pm 13 \mu\text{M}$	yes
	$120 \pm 14 \mu\text{M}$	$820 \pm 100 \mu\text{M}$	yes
	$53 \pm 4.2 \mu\text{M}$	$410 \pm 65 \mu\text{M}$	yes
	$37 \pm 9.4 \mu\text{M}$	$220 \pm 49 \mu\text{M}$	yes

	$9.1 \pm 0.53 \mu\text{M}$	$65 \pm 14 \mu\text{M}$	yes
	$12 \pm 2.4 \mu\text{M}$	$150 \pm 8.4 \mu\text{M}$	yes
	$120 \pm 15 \mu\text{M}$	$110 \pm 19 \mu\text{M}$	no
	$33 \pm 5.6 \mu\text{M}$	$110 \pm 6.5 \mu\text{M}$	yes
	$73 \pm 4.0 \mu\text{M}$	$380 \pm 7.8 \mu\text{M}$	yes
	$180 \pm 6.0 \mu\text{M}$	$200 \pm 29 \mu\text{M}$	no
	$11 \pm 0.29 \mu\text{M}$	$64 \pm 11 \mu\text{M}$	yes
	$42 \pm 8.7 \mu\text{M}$	$160 \pm 7.6 \mu\text{M}$	yes
	$17 \pm 3.6 \mu\text{M}$	$180 \pm 6.9 \mu\text{M}$	yes

	$27 \pm 7.2 \mu\text{M}$	$220 \pm 34 \mu\text{M}$	yes
	$100 \pm 9.7 \mu\text{M}$	$550 \pm 61 \mu\text{M}$	yes
	$59 \pm 16 \mu\text{M}$	$65 \pm 9.8 \mu\text{M}$	no
	$26 \pm 4.9 \mu\text{M}$	$240 \pm 15 \mu\text{M}$	yes
	$22 \pm 2.6 \mu\text{M}$	$95 \pm 8.0 \mu\text{M}$	yes
	$49 \pm 2.9 \mu\text{M}$	$260 \pm 49 \mu\text{M}$	yes
	$58 \pm 7.8 \mu\text{M}$	$630 \pm 75 \mu\text{M}$	yes
	$81 \pm 7.4 \mu\text{M}$	$160 \pm 9.5 \mu\text{M}$	yes

	$50 \pm 1.3 \mu\text{M}$	$310 \pm 23 \mu\text{M}$	yes
	$29 \pm 3.8 \mu\text{M}$	$230 \pm 11 \mu\text{M}$	yes
	$37 \pm 5.9 \mu\text{M}$	$240 \pm 8.7 \mu\text{M}$	yes
	$63 \pm 6.5 \mu\text{M}$	$370 \pm 23 \mu\text{M}$	yes
	$35 \pm 3.7 \mu\text{M}$	$110 \pm 12 \mu\text{M}$	yes
	$82 \pm 5.6 \mu\text{M}$	$160 \pm 12 \mu\text{M}$	yes
	$29 \pm 4.3 \mu\text{M}$	$260 \pm 32 \mu\text{M}$	yes
	$31 \pm 4.1 \mu\text{M}$	$97 \pm 6.4 \mu\text{M}$	yes
	$26 \pm 1.9 \mu\text{M}$	$92 \pm 8.0 \mu\text{M}$	yes

	$20 \pm 2.7 \mu\text{M}$	$290 \pm 7.5 \mu\text{M}$	yes
	$72 \pm 4.9 \mu\text{M}$	$380 \pm 29 \mu\text{M}$	yes

^a The range listed represents 95% confidence interval.
^b Compounds that exhibit competitive inhibition are boxed above.

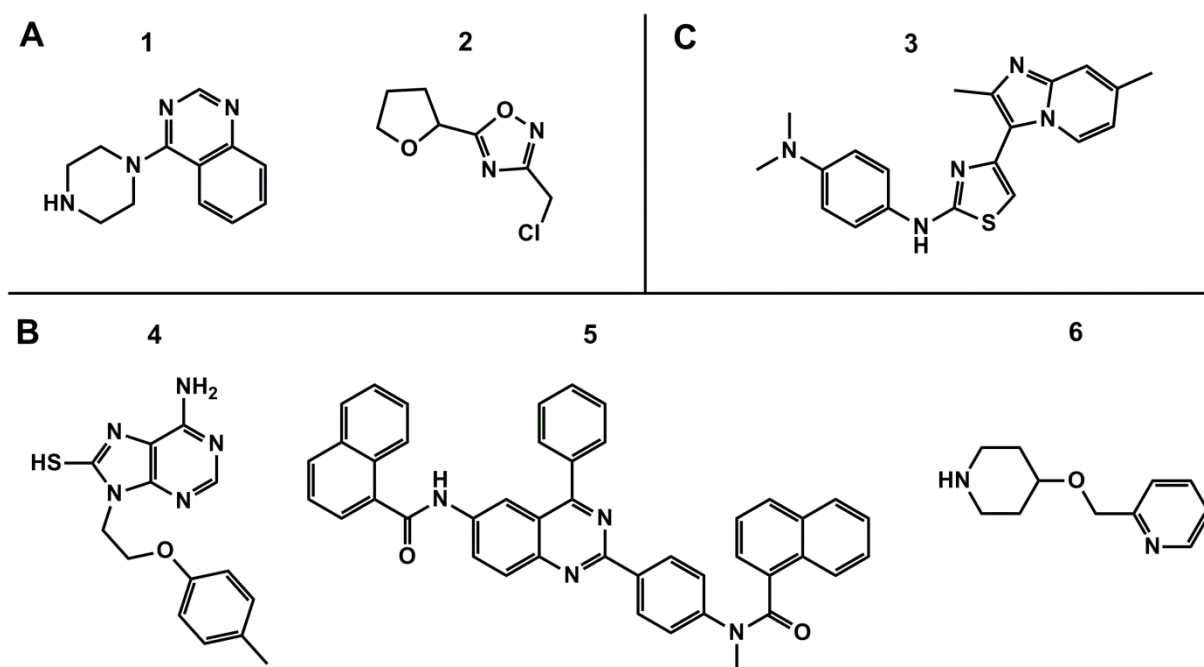


FIGURE 3-2. Compounds displaying competitive inhibition against *Mtb* ATP sulfurylase (CysNC•CysD). **A)** Compounds that bind in the GTP binding site. **B)** Compounds that bind in the ATP binding site. **C)** A compound that does not compete in either nucleotide binding site.

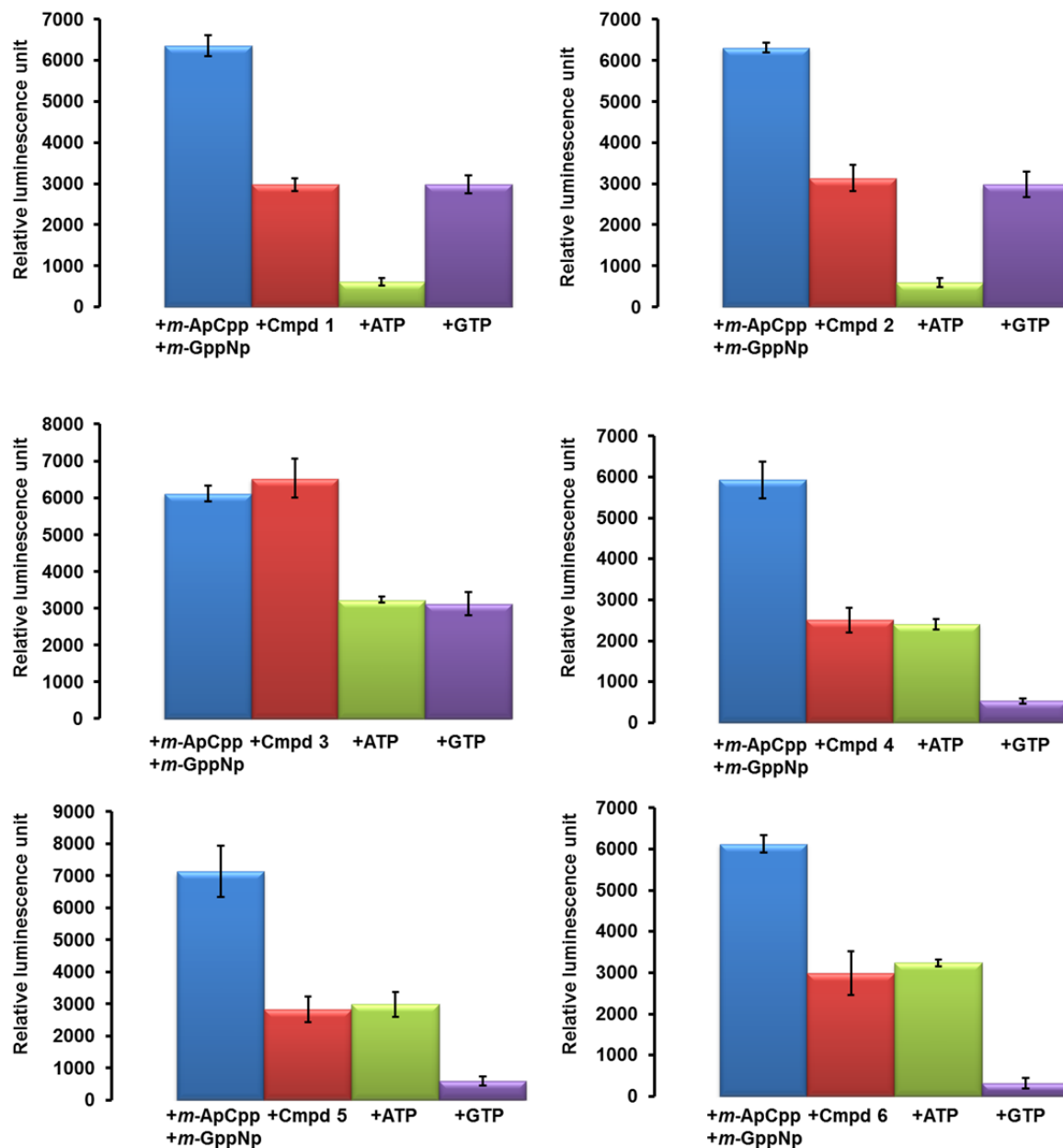


FIGURE 3-3. Competitive binding assay elucidates the binding sites of the 6 lead compounds. The first bar indicates the fluorescence level of truncated *Mtb* ATP sulfurylase incubated with *mant*-ApCpp and *mant*-GppNHp. In the second step, the lead compound out-competes one of the nucleotide binding sites, resulting in a decrease of fluorescence intensity. In the final step, ATP or GTP is added. For compound **1**, addition of ATP results in further decrease of fluorescence, which suggests that ATP out-competes *mant*-ApCpp and not compound **1**. The finding that compound **1** occupies the GTP pocket is corroborated by the addition of GTP in the final step. In this scenario, GTP out-competes compound **1**, resulting in no significant change in fluorescence. The summary of the results and categorization of the compounds are shown in **Figure 3-2**.

Lead compounds are discriminatory against eukaryotic ATP sulfurylases

To probe the specificity of the lead compounds, two eukaryotic organisms (*Homo sapiens* and *Saccharomyces cerevisiae*) and a prokaryotic organism (*Pseudomonas syringae*) were selected. As stated previously, eukaryotic homologs of ATPS do not couple the sulfurylation reaction with GTP hydrolysis. Indeed, lead compounds that were GTP antagonists showed no activity against *H. sapiens* and *S. cerevisiae* ATPS (**Table 1**). Compound **3**, the allosteric inhibitor, also specifically inhibit *P. syringae* and *Mtb* ATPS. ATP antagonists **3**, **4** and **5** show weak potency across species.

TABLE 3-2. GTP antagonists exhibit selectivity for prokaryotic homologs of ATP sulfurylase

Organisms	1 ^a	2 ^a	3 ^b	4 ^c	5 ^c	6 ^c
<i>M. tuberculosis</i>	5.7 ± 1.3	59 ± 16	7.2 ± 0.9	57 ± 9.6	180 ± 6.0	120 ± 15
<i>P. syringae</i>	13 ± 2.2	87 ± 9.3	68 ± 5.3	36 ± 3.2	180 ± 31	160 ± 8.8
<i>H. sapiens</i>	> 1000	> 1000	> 1000	89 ± 12	350 ± 29	260 ± 32
<i>S. cerevisiae</i>	> 1000	> 1000	> 1000	72 ± 9.6	340 ± 38	400 ± 8.0

^aCompounds **1** and **2** are GTP antagonists and showed no activity against eukaryotic ATPS. ^bCompound **3** is an allosteric inhibitor and exhibits selectivity between eukaryotic and prokaryotic ATPS. ^cCompounds **4**, **5** and **6** are ATP antagonists and display weak potency across species.

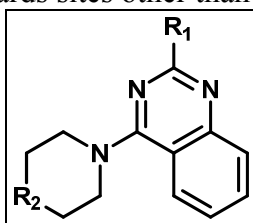
Analyzing the structure activity relationship by probing derivatives of the lead compounds

Compounds **1**, **2**, and **3** exhibited excellent specificity for prokaryotic ATP sulfurylase over eukaryotic homologs. Commercially available compounds from Chembridge (San Diego, CA) whose structure differ by one functional group from parent compounds **1** and **3** were purchased to perform structure activity relationship (SAR) analysis.

Structure activity relationship of compound 1

Compound **1** consists of a quinazoline core connected to a piperazine moiety via the C-4 position. There are many sites amenable to derivatization, and the derivatives ascertain the SAR of C-2 position (R₁) as well as the importance of the terminal nitrogen on the piperazine ring (**Figure 3-4**). All derivatives contain either a phenyl or heterocyclic ring at the R₁ position. Giving that none of the derivatives shows higher potency, no further optimization should be done at this position. The presence of a halide

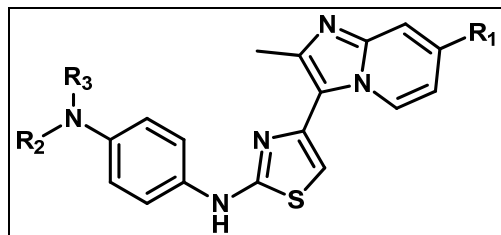
substituent on the phenyl group, completely abolish inhibitory activity (compounds **1-15** to **1-20**). The presence of a methyl group on the phenyl ring also decreases the activity (**1-7** vs. **1-12**, **1-8**, vs. **1-13**, **1-9**, vs. **1-14**). In addition, puridine substitution is slightly favored over phenyl substitution (**1-1** to **1-6**, vs. **1-7** to **1-11**). The position of the nitrogen on the puridine has no effect on the activity. Among all R₂ substituents, substituting nitrogen with carbon eliminates activity (**1-3** vs. **1-1**; **1-6** vs. **1-4**; **1-10** and **1-11** vs. **1-7** and **1-8**; **1-14** vs. **1-12** and **1-13**). Substituting nitrogen with oxygen also suffers decrease in activity. Taken together, parent compound **1** has the highest activity, and that future SAR studies should be geared towards sites other than R₁ and R₂.



Compound	R ₁	R ₂	IC ₅₀ (μM)
1	H	NH	5.7 ± 1.3
1-1		N-Me	58 ± 7.3
1-2		O	310 ± 8.0
1-3		CH-Me	> 1000
1-4		N-Me	81 ± 6.4
1-5		O	290 ± 27
1-6		CH-Me	> 1000
1-7		N-Me	130 ± 23
1-8		N-Et	220 ± 39
1-9		O	400 ± 69
1-10		CH-Me	> 1000
1-11		CH ₂	> 1000
1-12		N-Me	170 ± 38
1-13		N-Et	410 ± 51
1-14		O	620 ± 81
1-15		N-Me	> 1000
1-16		N-Et	> 1000
1-17		O	> 1000
1-18		N-Me	> 1000
1-19		N-Et	> 1000
1-20		O	> 1000

FIGURE 3-4. Sites of derivatization for **1**. The substituents from the parent compound are bolded and underlined.

Structure activity relationship (SAR) of compound 3



Compound	R ₁	R ₂	R ₃	IC ₅₀ (μM)
<u>3</u>	<u>Me</u>	<u>Me</u>	<u>Me</u>	<u>7.2 ± 0.9</u>
3-1	Me	H	H	58 ± 4.1
3-2	H	H	H	95 ± 7.0
3-3	Me	Et	Et	210 ± 17
3-4	H	Et	Et	300 ± 25
3-5	Me	Ac	H	> 1000
3-6	H	Ac	H	> 1000
3-7	Me	O	O	> 1000
3-8	H	O	O	> 1000

FIGURE 3-5. Sites of derivatization for **3**. The substituents from the parent compound are bolded and underlined.

To study the structure activity relationship, 8 derivatives of **3** were probed (**Figure 3-5**). The C-7 position at the imidazo[1,2- α]pyridine core shows preference for methyl over hydrogen as compound **3-1** has lower IC₅₀ value compared with **3-2** (58 μM vs. 95 μM) and **3-3** also has lower IC₅₀ value to **3-4** (210 μM vs. 300 μM). In addition, the nitrogen exhibits preference for hydrogen at the R₂ and R₃ positions over ethyl group. Compound **3-2** is more potent than **3-4** (95 μM vs. 300 μM), and compound **3-1** is more active than **3-3** (58 μM vs. 210 μM). However, when an *N*-acetamide or a nitro group is present, the activity of the compound completely abolishes (compounds **3-5**, **3-6**, **3-7**, and **3-8**). Taken together, the parent compound **3** is the most active relative to its derivatives.

Conclusions

In this chapter, we present the follow up validation following the high throughput screen. The hit compounds identified by the high throughput screen were subjected to a battery of assays. First, IC₅₀ values at different enzyme concentrations were measured to determine if aggregate formation was a plausible mechanism for inhibition. Of the 45 hit compounds, 6 were shown to be competitive inhibitors. Next, utilizing fluorescent non-hydrolyzable nucleotide analogs, we were able to determine the binding mode of the 6 lead

compounds: two were GTP antagonists, three were ATP antagonists, and one seem to bind at a site distal to the active site and were categorized as an allosteric inhibitor.

Knowing the binding mechanism of the lead compounds, specificity were determined by measuring IC_{50} values of ATP sulfurylase from other species. Indeed, since GTPase domain is absent from all eukaryotic ATP sulfurylase, GTP antagonists showed specificity toward prokaryotic ATP sulfurylase. The allosteric inhibitor also exhibited specificity. However, ATP antagonists demonstrated weak activity across all ATP sulfurylase homologs.

Lastly, structure activity relations were conducted as a means to improve potency. None of the derivatives were more potent than the parent compound, which suggest that future optimization should focus on the substituents not presented in this chapter. Interestingly, the observation that small molecules can discriminate eukaryotic ATP sulfurylase from prokaryotic sulfurylase lends more credibility that the absence of cross-reactivity makes the sulfate assimilation pathway an excellent drug target.

Materials and Methods

Materials

Fluorescent non-hydrolyzable nucleotides, 2'/3'-O-(N-Methyl-anthraniloyl)-guanosine-5'-[(β,γ)-imido]triphosphate (*mant*-GppNHp) and 5 μ M 2'/3'-O-(N-Methyl-anthraniloyl)-adenosine-5'-[(α,β)-imido] triphosphate (*mant*-ApCpp) were from Jena Bioscience (Jena, Germany). The derivative compounds were from ChemBridge Corporation (San Diego, CA).

Expression and purification of Mtb CysN•CysD in *E. coli*

pET28b_CysN and pET21a_CysD were co-transformed into *E. coli* strain BL21(DE3). Selected double transformants were used to streak for single colonies. The single colonies were used to inoculate 4-L cultures of LB medium containing 100 mg/L kanamycin and 100 mg/L ampicillin. The cultures were incubated at 37 °C for approximately 4 h with shaking at 250 rpm until an OD_{600} of 0.6 was reached. Protein expression was induced by the addition of isopropyl β -D-thiogalactoside (IPTG) to a final concentration of 100 μ M for an additional 16 h at 18 °C. *E. coli* cells were harvested by centrifugation (6000 rpm, 4 °C, 15 min). The pelleted cells were resuspended in 15 ml of lysis buffer (50 mM Tris [pH 7.5], 0.5 M NaCl, 10% glycerol [v/v], 15 mM imidazole, 2 mM β -mercaptoethanol and 1 complete ultra, EDTA-free protease inhibitor cocktail tablet (Roche) at 4 °C. Cells were lysed by ultrasonication (Misonix Sonicator 3000). The cell lysate was cleared by centrifugation (18,500 rpm, 4 °C, 20 min). The resulting supernatant was loaded onto a Ni-NTA column pre-equilibrated with lysis buffer supplemented with 25 mM imidazole overnight at 4 °C. Proteins were washed with lysis buffer supplemented with 100 mM imidazole and subsequently eluted with a gradient of 500 mM imidazole and selected fractions were pooled.

Measurement of IC₅₀

Hit compounds were dispensed in flat-bottom white 96-well polypropylene assay plates (Corning). Each compound was serially diluted 2-fold in reaction buffer (final concentration 35 μ M ATP [$1 \times K_M$], 13 μ M GTP [$1 \times K_M$], 1.0 mM Na₂SO₄, 2.0 mM MgCl₂, 50 mM HEPES [pH 8.0], 2% DMSO), with final compound concentration ranging from 1 mM to 0.98 μ M. Reaction buffer was added in place of the compound for negative controls, heat-killed *Mtb* ATPS was used for positive controls. *Mtb* ATPS (final concentration 1.2 μ M) was added to the mixture and allowed to react for 30 min in room temperature. Reactions were terminated with the addition of 1:1 (v/v) Kinase-Glo+ (Promega) and equilibrated for 10 min on a plate shaker. Luminescence intensity was measured by SpectraMax M3 (Molecular Devices). IC₅₀ values were calculated by fitting the data by non-linear regression analysis to a competitive inhibition model using the KaleidaGraph software version 3.6.

Nucleotide pocket binding Assay

Mtb ATPS was equilibrated using a plate shaker for 5 min in room temperature with 5 μ M 2'/3'-O-(N-Methyl-anthraniloyl)-guanosine-5'-[(β,γ)-imido]triphosphate (*mant*-GppNHp) and 5 μ M 2'/3'-O-(N-Methyl-anthraniloyl)-adenosine-5'-[(α,β)-imido]triphosphate (*mant*-ApCpp) in reaction buffer (1.0 mM Na₂SO₄, 2.0 mM MgCl₂, 50 mM HEPES [pH 8.0]) and 1.2 μ M *Mtb* ATPS. The assay mixture was added to a clear flat-bottom 96-well assay plate (Greiner). 1:1 [v/v] of 100 μ M hit compound in reaction buffer was added to the assay mixture and equilibrated using a plate shaker for 5 min in room temperature. 5 mM of ATP or GTP in reaction buffer was added to the resulting assay mixture from previous step and equilibrated. Control lanes were added reaction buffer without the hit compound and ATP or GTP. Reaction mixture without *Mtb* ATPS served as a baseline for fluorescent reading. Fluorescence intensity was measured by SpectraMax M3 (Molecular Devices) at 448 nm.

Comparative Activity Assay

The Kinase-Glo+ reagent (Promega) was used to measure the ATP consumption by *Mtb* ATP sulfurylase. A standard reaction mixture contained 35 μ M ATP [$1 \times K_M$], 13 μ M GTP [$1 \times K_M$], , 1.0 mM Na₂SO₄, 2.0 mM MgCl₂, 1 mM 50 mM HEPES buffer [pH 8.0], 1.2 μ M *Mtb* ATP sulfurylase. The reaction was allowed to proceed in room temperature for 30 min and quenched with 1:1 [v/v] of Kinase-Glo+ reagent. In the 96-well format, white, flat-bottom assay plates (Greiner) were used. 50 μ L of reaction volume was added with 50 μ L Kinase-Glo+ reagent. After a 10 min incubation for Kinase-Glo+ reagent to react and the luminescence signal to equilibrate, the luminescence was determined by a SpectraMax M3 (Molecular Devices). Standard ATP curve was generated by serially diluting 100 μ M ATP to 0.78 μ M.

References

1. McGovern, S.L., et al., *A specific mechanism of nonspecific inhibition*. J Med Chem, 2003. **46**(20): p. 4265-72.
2. McGovern, S.L. and B.K. Shoichet, *Kinase inhibitors: not just for kinases anymore*. J Med Chem, 2003. **46**(8): p. 1478-83.
3. McGovern, S.L., et al., *A common mechanism underlying promiscuous inhibitors from virtual and high-throughput screening*. J Med Chem, 2002. **45**(8): p. 1712-22.
4. Seidler, J., et al., *Identification and prediction of promiscuous aggregating inhibitors among known drugs*. J Med Chem, 2003. **46**(21): p. 4477-86.
5. Mougous, J.D., et al., *Molecular basis for G protein control of the prokaryotic ATP sulfurylase*. Mol Cell, 2006. **21**(1): p. 109-22.
6. Hiratsuka, T., *New ribose-modified fluorescent analogs of adenine and guanine nucleotides available as substrates for various enzymes*. Biochim Biophys Acta, 1983. **742**(3): p. 496-508.
7. Hiratsuka, T., *A chromophoric and fluorescent analog of GTP, 2',3'-O-(2,4,6-trinitrocyclohexadienylidene)-GTP, as a spectroscopic probe for the GTP inhibitory site of liver glutamate dehydrogenase*. J Biol Chem, 1985. **260**(8): p. 4784-90.
8. Wang, J.L., et al., *A conformational transition in the adenylyl cyclase catalytic site yields different binding modes for ribosyl-modified and unmodified nucleotide inhibitors*. Bioorg Med Chem, 2007. **15**(8): p. 2993-3002.
9. Bujalowski, W. and M.J. Jezewska, *Kinetic mechanism of nucleotide cofactor binding to Escherichia coli replicative helicase DnaB protein. stopped-flow kinetic studies using fluorescent, ribose-, and base-modified nucleotide analogues*. Biochemistry, 2000. **39**(8): p. 2106-22.
10. Strelow, J., et al., *Mechanism of Action assays for Enzymes*. 2004.
11. Pinto, C., et al., *Structure-activity relationships for the interactions of 2'- and 3'-(O)-(N-methyl)anthraniloyl-substituted purine and pyrimidine nucleotides with mammalian adenylyl cyclases*. Biochem Pharmacol, 2011. **82**(4): p. 358-70.
12. Pommier, Y. and C. Marchand, *Interfacial inhibitors: targeting macromolecular complexes*. Nat Rev Drug Discov, 2012. **11**(1): p. 25-36.
13. Changeux, J.P., *50th anniversary of the word "allosteric"*. Protein Sci, 2011. **20**(7): p. 1119-24.

14. Christopoulos, A., *Allosteric binding sites on cell-surface receptors: novel targets for drug discovery*. Nat Rev Drug Discov, 2002. **1**(3): p. 198-210.

Chapter 4: Characterization of the lead compounds' *in vivo* activity and specificity against *Mtb* and other pathogenic bacteria

Introduction

After an oral drug is administered, it undergoes many chemical transformations in the digestive tract, blood stream, and finally to the site of interest. The interaction between the drug and the body is bilateral, and can be defined by two terms: pharmacokinetics, which is defined as “what the body does to the drug”, and pharmacodynamics, which is defined as “what the drug does to the body” [1-6]. During the early stages of drug development, pharmacodynamics, which also accounts for the toxicity of the drug, is more relevant. In particular, during the development of antibiotics, the bactericidal effect cannot also illicit cytotoxicity in mammalian cells. Thus, emphasis is often placed on specificity of the compound and the minimization of cross-reactivity between homologous targets [7-10].

The six lead compounds' *in vitro* activity and selectivity was established in the last chapter. In this chapter, we investigated the ability for the lead compounds to inhibit growth *in vivo*. In addition to *Mtb*, *B. subtilis* (Gram positive), *E. coli* (Gram negative), and yeast (eukaryotic) were subjected to incubation with the lead compound in absence of cysteine and methionine to challenge the sulfate assimilation pathway. In this condition, inhibition of ATP sulfurylase effectively creates a “chemical auxotroph”. To eliminate the possibility that the compounds possess off-target activity and exhibit board-spectrum toxicity, the cytotoxicity of mammalian Vero cells were investigated.

Results and Discussion

Compounds 1 and 2 exhibit cytotoxicity in Vero cell line

To investigate the cytotoxicity in mammalian cells, Vero cells (CCL-81, ATCC) were treated with lead compounds from 0.98 μM to 2,000 μM to determine the dose response in relation to growth inhibition (**Figure 4-1**). The viability of the cells was measured by alamarBlue assay (Invitrogen), which correlates cell number with fluorescence intensity [11, 12]. Geneticin from 2.4 $\mu\text{g}/\text{mL}$ to 5.0 mg/mL was used as a positive control. The fluorescent intensity measured from geneticin at 5.0 mg/mL was to normalize as 100% cell growth inhibition. Compound **1** exhibits dose-dependent cytotoxicity, starting at 4 μM (minimal inhibitory concentration, MIC), while the toxicity profile of compound **2** shows no dose-dependency. Treatment of geneticin showed full inhibition at 39 $\mu\text{g}/\text{ml}$, and the result is consistent with the concentration (50 $\mu\text{g}/\text{ml}$) used for the selection of geneticin-resistant cell lines. Compounds **3**, **4**, **5**, and **6** do not show cytotoxicity below 2 mM. Compound **2** exhibited moderate toxicity from 1 μM to 1 mM in a non-dose dependent manner.

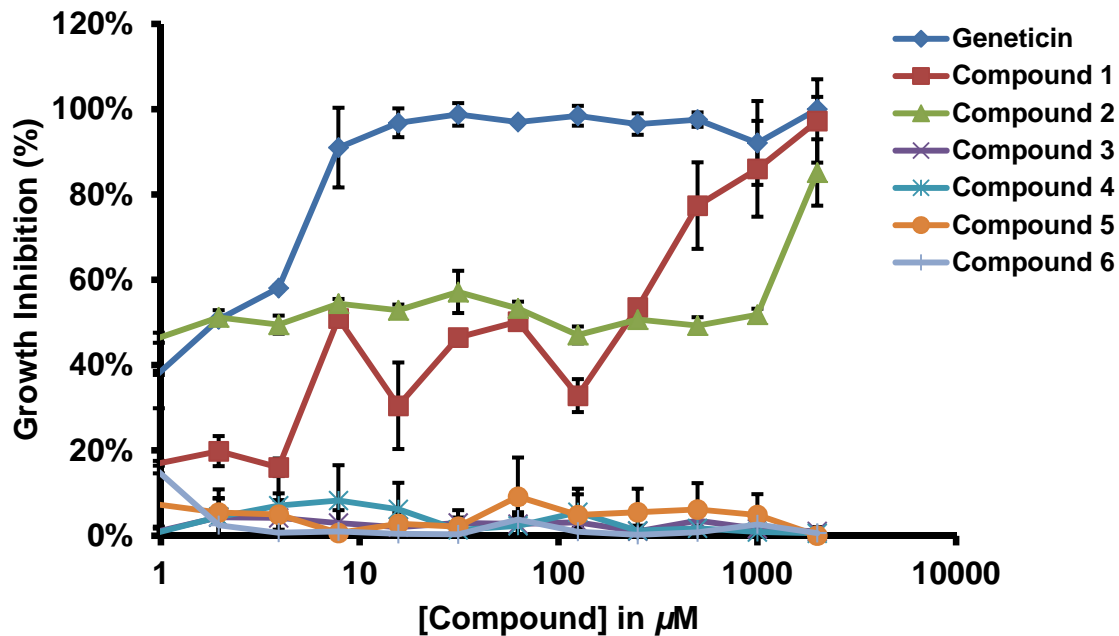


FIGURE 4-1. Cytotoxicity of the 6 lead compounds. Geneticin was used as the positive control, and the fluorescence intensity at 5 mg/mL was normalized as 100% growth inhibition. Compound 1 shows dose-dependent cytotoxicity starting at 4 μM (MIC).

Lead compounds do not inhibit growth of Saccharomyces cerevisiae below 2 mM

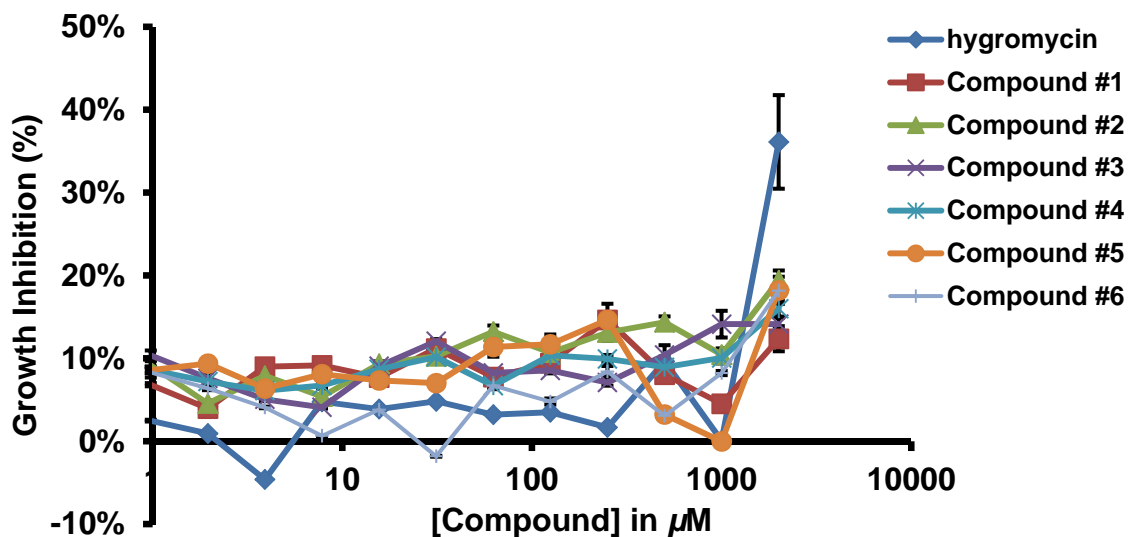


FIGURE 4-2. Lead compounds do not inhibit growth in *Saccharomyces cerevisiae* cultures less than 2,000 μM . Hygromycin was used as a positive control and has moderate inhibitory activity at 200 $\mu\text{g/ml}$.

The potential for growth inhibition in yeast (*Saccharomyces cerevisiae*) was investigated (**Figure 4-2**). Yeast cultures growing in complete minimal dropout medium without cysteine and methionine were treated with the 6 lead compounds at concentrations from 0.98 μM to 2,000 μM . Hygromycin, a broad-spectrum antibiotic which inhibits protein synthesis [13] was used as a positive control at concentrations from 0.02 $\mu\text{g/ml}$ to 50 $\mu\text{g/ml}$ was used. Hygromycin showed moderate growth inhibition at 50 $\mu\text{g/ml}$, which is at the lower range for selection (50 to 200 $\mu\text{g/ml}$). All 6 lead compounds did not inhibit growth below 2,000 μM .

In vivo inhibitory activity against Gram negative pathogen E. coli and Gram positive pathogen Bacillus subtilis

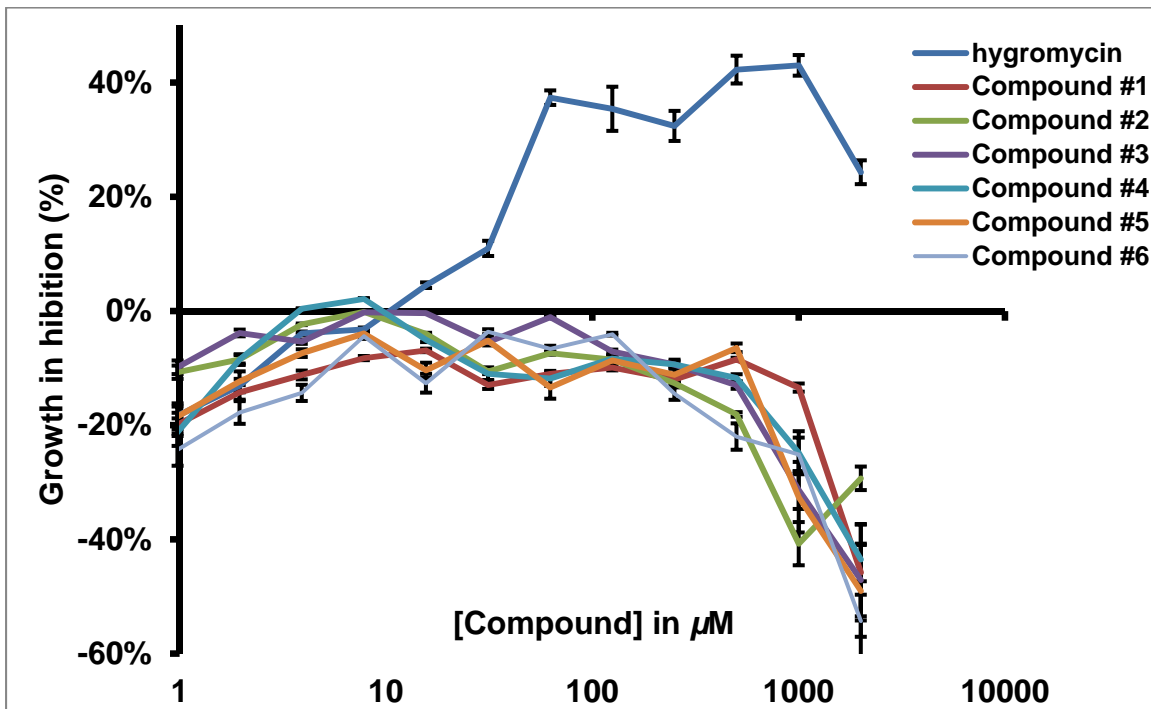


FIGURE 4-3. The growth inhibitory activity of the lead compounds against *E. coli* is inconclusive. Hygromycin was used as a positive control.

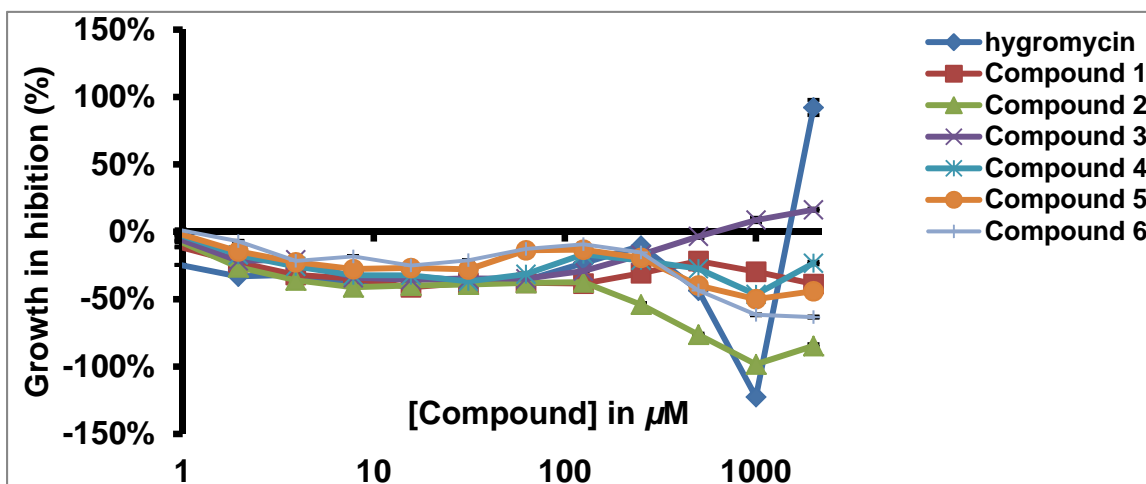


FIGURE 4-4. The growth inhibitory activity of the lead compounds against *B. subtilis* is inconclusive. Hygromycin was used as a positive control.

To assess the potential for the lead compounds to inhibit growth under restrictive conditions without cysteine and methionine, cultures of *E. coli* and *Bacillus subtilis* were treated the lead compound at concentrations from 0.98 μM to 2,000 μM (**Figure 4-3** and **Figure 4-4**). Hygromycin was used as a positive control at concentrations from 0.02 $\mu\text{g/ml}$ to 50 $\mu\text{g/ml}$. Due to the low growth in 96-well plates, some OD₆₀₀ readings were out of the linear range of the instrument. Therefore, no conclusions can be drawn from the experiment.

In vivo inhibitory activity against *Mtb*

The growth inhibitory activity of the lead compounds was examined in WT H37Rv *Mtb* (**Figure 4-5**). Cultures was grown in Sauton's minimal media without supplementing cysteine and methionine. Isoniazid, a front-line TB drug was used as a positive control [14-16] from concentrations of 0.49 ng/mL to 1 $\mu\text{g/mL}$. The literature reported MIC is approximately 0.2 $\mu\text{g/mL}$ [17-21]. Isoniazid is shown to have moderate potency across all concentrations. Compound **1** inhibits growth in a dose-dependent manner starting at 125 μM . At 500 μM , all compounds exhibit growth inhibition. However, only compounds **1** and **5** achieve 50% inhibition at 2 mM concentration. Since **1** also inhibits growth of Vero cells, the possibility of off-target effect cannot be eliminated. Compound **5**, which has an MIC of approximately 500 μM is a promising lead. Further optimization will be needed to improve the MIC by evading a plethora of efflux pumps in *Mtb* as well as better intracellular access [22-27].

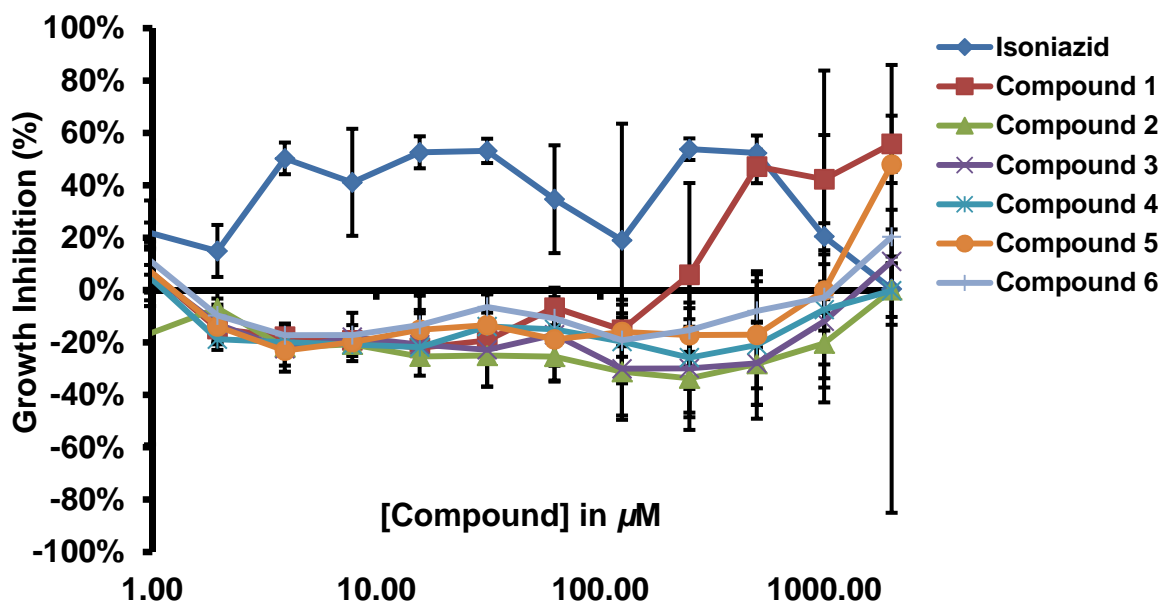


FIGURE 4-5. Lead compounds **1** and **5** inhibit growth of *Mtb* cultures at 125 μM and 500 μM , respectively. Isoniazid was used as a positive control and has moderate inhibitory across all concentrations.

Conclusions

In this chapter, we present the investigation of *in vivo* activities of the six lead compounds. We examined the cytotoxic profiles of the lead compounds in mammalian Vero cell line. Compound **1** exhibits dose-dependent inhibition of growth starting at 125 μM . Compound **2** also displayed activity to inhibit growth at 2 mM. Other compounds do not show cytotoxicity below 2 mM. Next, we test the lead compounds activity against Gram negative (*E. coli*) and Gram positive (*Bacillus subtilis*) pathogens. Unfortunately, due to the low growth in minimal media resulting in OD₆₀₀ readings below the linear range of the instrument, no conclusions can be drawn. Lastly, we assess the *in vivo* activities in *Mtb*. Compound **1** has an observed MIC of 125 μM . However, at this concentration, **1** is also cytotoxic, rendering it undesirable for further development. Compound **5**, which exhibits 50% growth inhibition at 2 mM, has an observed MIC of 500 μM . Compound **5** therefore is the leading candidate for lead optimization. From **Chapter 3**, it has broad-spectrum activity against both prokaryotic and eukaryotic ATP sulfurylase homologs. Future effort in synthesizing derivatives should be focused on increasing the specificity for *Mtb* ATP sulfurylase, while at the same time decreasing the affinity for eukaryotic ATP sulfurylase. In addition, compound **5** is an ATP antagonist, it is conceivable that cross-reactivity with kinases is a cause for concern. In summary, with the discovery of compound **5**, we established a foundation for initiating a latent-TB drug discovery program. In addition, due to its low cytotoxicity, it also has the potential to be a tool for studying the sulfate assimilation pathway in macrophage infection models.

Materials and Methods

Minimum inhibitor concentration (MIC) determination

WT H37Rv *Mtb* was grown to mid-log phase in 50 mL media in roller bottles. Clumps were removed by centrifugation and washed in Sauton's media (0.5 g KH₂PO₄, 0.5 g MgSO₄, 2 g citric acid, 0.05 g ferric ammonium citrate, 60 mL glycerol, 4 g *L*-asparagine, 0.1 mL of 1% ZnSO₄, 2.5 mL of 20% Tween-80, and 2% DMSO, in 1 L H₂O) three times. The bacteria were diluted to an OD₆₀₀ of 0.2. Two fold serial dilutions of each chemical inhibitor were set up in clear, flat-bottom 96-well plates in 20 μ L from 2 mM to 0.98 μ M. Each well was inoculated with 80 μ L of WT H37Rv. Plates were parafilm and placed into a sealed Tupperware container containing damp towels to prevent evaporation. Plates were incubated for 7 days at 37 °C. Plates were fixed with 100 μ L 10 % formalin in buffered PBS and OD₆₀₀ was read on a VersaMax UV/Vis plate reader (Molecular Devices).

E. coli was grown to mid-log phase in 50 mL LB media in roller bottles. Clumps were removed by centrifugation and washed in M9 minimal media (12.8 g Na₂HPO₄•7H₂O, 3 g KH₂PO₄, 0.5 g NaCl, 1 g NH₄Cl, 2 mM MgSO₄, 0.1 mM CaCl₂, 0.5% glucose, 2% DMSO, in 1 L H₂O) three times. The bacteria were diluted to an OD₆₀₀ of 0.2. Two fold serial dilutions of each chemical inhibitor were set up in clear, flat-bottom 96-well plates in 20 μ L from 2 mM to 0.98 μ M. Each well was inoculated with 80 μ L culture. Plates were parafilm and placed into a sealed Tupperware container containing damp towels to prevent evaporation. Plates were incubated for 2 days at 37 °C. OD₆₀₀ was read on a SpectraMax M3 UV/Vis plate reader (Molecular devices).

Bacillus subtilis was grown to mid-log phase in 50 mL LB media in roller bottles. Clumps were removed by centrifugation and washed in M9 minimal media (12.8 g Na₂HPO₄•7H₂O, 3 g KH₂PO₄, 0.5 g NaCl, 1 g NH₄Cl, 2 mM MgSO₄, 0.1 mM CaCl₂, 0.5% glucose, 2% DMSO, in 1 L H₂O) three times. The bacteria were diluted to an OD₆₀₀ of 0.2. Two fold serial dilutions of each chemical inhibitor were set up in clear, flat-bottom 96-well plates in 20 μ L from 2 mM to 0.98 μ M. Each well was inoculated with 80 μ L culture. Plates were parafilm and placed into a sealed Tupperware container containing damp towels to prevent evaporation. Plates were incubated for 2 days at 37 °C. OD₆₀₀ was read on a SpectraMax M3 UV/Vis plate reader (Molecular devices).

Saccharomyces cerevisiae was grown to mid-log phase in 50 mL YPD media in roller bottles. Clumps were removed by centrifugation and washed in complete minimal (CM) dropout medium (1.7 g YNB-AA/AS, 5 g (NH₄)₂SO₄, 20 g dextrose, 40 μ g/mL adenine, 20 μ g/mL *L*-arginine, 100 μ g/mL *L*-aspartic acid, 100 μ g/mL *L*-glutamic acid, 20 μ g/mL *L*-histidine, 60 μ g/mL *L*-leucine, 30 μ g/mL *L*-lysine, 50 μ g/mL *L*-phenylalanine, 375 μ g/mL *L*-serine, 200 μ g/mL *L*-threonine, 40 μ g/mL *L*-tryptophan, 30 μ g/mL, 150 μ g/mL *L*-valine, 20 μ g/mL uracil in 1 L H₂O) three times. The yeast culture was diluted to an OD₆₀₀ of 0.2. Two fold serial dilutions of each chemical inhibitor were set up in clear, flat-bottom 96 well plates in 20 μ L from 2 mM to 0.98 μ M. Each well was inoculated with 80 μ L culture. Plates were parafilm and placed into a sealed Tupperware container containing damp towels to prevent evaporation. Plates were

incubated for 2 days at 37 °C. OD₆₀₀ was read on a SpectraMax M3 UV/Vis plate reader (Molecular devices).

Cytotoxicity measurements in Vero Cells

Toxicity of the compounds were tested in Vero cells (CCL-81, ATCC) using the alamarBlue assay (DAL1100, Life Technologies). Vero cells were cultured based on ATCC protocols and passaged three times to restore normal growing conditions. Two fold serial dilutions of each chemical inhibitor were set up in sterile, clear, flat-bottom 96-well plates in 20 μ L from 2 mM to 0.98 μ M concentration. Geneticin was used as a positive control and was diluted from 5.0 mg/ml to 2.4 μ g/ml. Passaged cells were diluted 1:10 in complete ATCC's Eagle's Essential Medium [ATCC's Eagle's Minimal Essential Medium (30-2003, ATCC), supplemented with 10% [v/v] fetal bovine serum], and 80 μ L was inoculated onto each well. The cells were incubated with the compounds for 24 h. 10 μ L of the alamarBlue assay was added to each well and incubated for an additional 6 h until the signal was stabilized. Experiments were carried out in triplicate. The fluorescence (Excitation: 560 nm, emission: 590 nm) intensity was read on a SpectraMax M3 UV/Vis plate reader (Molecular devices). The fluorescence correlates positively

References

1. Nightingale, C.H. and P. Carver, *Basic principles of pharmacokinetics*. Clin Lab Med, 1987. **7**(2): p. 267-78.
2. Benet, L.Z. and P. Zia-Amirhosseini, *Basic principles of pharmacokinetics*. Toxicol Pathol, 1995. **23**(2): p. 115-23.
3. Craig, W.A., *Choosing an antibiotic on the basis of pharmacodynamics*. Ear Nose Throat J, 1998. **77**(6 Suppl): p. 7-11; discussion 11-2.
4. Takimoto, C.H., *Basic pharmacokinetics and pharmacodynamic principles*. Cancer Treat Res, 2001. **106**: p. 85-101.
5. Mulla, H., *Understanding developmental pharmacodynamics: importance for drug development and clinical practice*. Paediatr Drugs, 2010. **12**(4): p. 223-33.
6. Schmidt, S., D. Gonzalez, and H. Derendorf, *Significance of protein binding in pharmacokinetics and pharmacodynamics*. J Pharm Sci, 2010. **99**(3): p. 1107-22.
7. Vugmeyster, Y., et al., *Pharmacokinetics and toxicology of therapeutic proteins: Advances and challenges*. World J Biol Chem, 2012. **3**(4): p. 73-92.
8. Pellegatti, M., *Preclinical in vivo ADME studies in drug development: a critical review*. Expert Opin Drug Metab Toxicol, 2012. **8**(2): p. 161-72.

9. Jorgensen, J.T., *A challenging drug development process in the era of personalized medicine*. Drug Discov Today, 2011. **16**(19-20): p. 891-7.
10. Gallo, J.M., *Pharmacokinetic/ pharmacodynamic-driven drug development*. Mt Sinai J Med, 2010. **77**(4): p. 381-8.
11. Nociari, M.M., et al., *A novel one-step, highly sensitive fluorometric assay to evaluate cell-mediated cytotoxicity*. J Immunol Methods, 1998. **213**(2): p. 157-67.
12. Nakayama, G.R., et al., *Assessment of the Alamar Blue assay for cellular growth and viability in vitro*. J Immunol Methods, 1997. **204**(2): p. 205-8.
13. Rao, R.N., et al., *Genetic and enzymatic basis of hygromycin B resistance in Escherichia coli*. Antimicrob Agents Chemother, 1983. **24**(5): p. 689-95.
14. Balcells, M.E., et al., *Isoniazid preventive therapy and risk for resistant tuberculosis*. Emerg Infect Dis, 2006. **12**(5): p. 744-51.
15. Panchagnula, R., et al., *Evaluation of bioequivalence of isoniazid and pyrazinamide in three and four drugs fixed dose combinations using WHO simplified protocol*. Pharmacol Res, 2003. **48**(4): p. 383-7.
16. Mitchison, D.A., *Antimicrobial therapy of tuberculosis: justification for currently recommended treatment regimens*. Semin Respir Crit Care Med, 2004. **25**(3): p. 307-15.
17. Bardarov, S., Jr., et al., *Detection and drug-susceptibility testing of M. tuberculosis from sputum samples using luciferase reporter phage: comparison with the Mycobacteria Growth Indicator Tube (MGIT) system*. Diagn Microbiol Infect Dis, 2003. **45**(1): p. 53-61.
18. Migliori, G.B., et al., *Diagnosis of multidrug-resistant tuberculosis and extensively drug-resistant tuberculosis: Current standards and challenges*. Can J Infect Dis Med Microbiol, 2008. **19**(2): p. 169-72.
19. Wichelhausen, R.H. and L.B. Robinson, *Drug-susceptibility testing by laboratories participating in cooperative studies on the chemotherapy of tuberculosis*. Am Rev Respir Dis, 1969. **99**(1): p. 1-7.
20. Kim, S.J., *Drug-susceptibility testing in tuberculosis: methods and reliability of results*. Eur Respir J, 2005. **25**(3): p. 564-9.
21. Dunbar, F.P., R. Davis, and M.B. Jefferies, *Drug-susceptibility testing in tuberculosis; a method using diluted bacterial suspensions for the indirect test*. Am Rev Tuberc, 1958. **77**(2): p. 350-5.

22. Van Bambeke, F., J.M. Michot, and P.M. Tulkens, *Antibiotic efflux pumps in eukaryotic cells: occurrence and impact on antibiotic cellular pharmacokinetics, pharmacodynamics and toxicodynamics*. J Antimicrob Chemother, 2003. **51**(5): p. 1067-77.
23. Srinivas, N.R., *Baicalin, an emerging multi-therapeutic agent: pharmacodynamics, pharmacokinetics, and considerations from drug development perspectives*. Xenobiotica, 2010. **40**(5): p. 357-67.
24. Machado, D., et al., *Contribution of Efflux to the Emergence of Isoniazid and Multidrug Resistance in Mycobacterium tuberculosis*. PLoS One, 2012. **7**(4): p. e34538.
25. Amaral, L., M. Martins, and M. Viveiros, *Enhanced killing of intracellular multidrug-resistant Mycobacterium tuberculosis by compounds that affect the activity of efflux pumps*. J Antimicrob Chemother, 2007. **59**(6): p. 1237-46.
26. Ollinger, J., et al., *Validation of the essential ClpP protease in Mycobacterium tuberculosis as a novel drug target*. J Bacteriol, 2012. **194**(3): p. 663-8.
27. Amaral, L. and M. Viveiros, *Why thioridazine in combination with antibiotics cures extensively drug-resistant Mycobacterium tuberculosis infections*. Int J Antimicrob Agents, 2012. **39**(5): p. 376-80.